I.O.S.

GEOCHEMISTRY OF THE NEAR SURFACE SEDIMENTS OF THE NARES ABYSSAL PLAIN

BY
M.S.N. CARPENTER, S. COLLEY,
H. ELDERFIELD, H.A. KENNEDY,
J. THOMSON AND T.R.S. WILSON

REPORT NO. 174
1983

OCEAN DISPOSAL OF HIGH LEVEL RADIOACTIVE WASTE
A RESEARCH REPORT PREPARED FOR THE DEPARTMENT
OF THE ENVIRONMENT

NATURAL ENVIRONMENT RESEARCH COUNCIL

INSTITUTE OF
OCEANOGRAPHIC
SCIENCES

INSTITUTE OF OCEANOGRAPHIC SCIENCES

Wormley, Godalming,
Surrey, GU8 5UB.
(0428 - 79 - 4141)

(Director: Dr. A.S. Laughton FRS)

Bidston Observatory,
Birkenhead,
Merseyside, L43 7RA.
(051 - 653 - 8633)

(Assistant Director: Dr. D.E. Cartwright)

Crossway,
Taunton,
Somerset, TA1 2DW.
(0823 - 86211)

(Assistant Director: M.J. Tucker)

When citing this document in a bibliography the reference should be given as follows:-

CARPENTER, M.S.N., COLLEY, S., ELDERFIELD, H., KENNEDY, H.A., THOMSON, J. & WILSON, T.R.S. 1983 Geochemistry of the near surface sediments of the Nares Abyssal Plain. *Institute of Oceanographic Sciences, Report*, No. 174, 66pp.

INSTITUTE OF OCEANOGRAPHIC SCIENCES

WORMLEY

Geochemistry of the near surface sediments of the Nares Abyssal Plain

by

M.S.N. Carpenter, S. Colley,
*H. Elderfield, *H.A. Kennedy,
J. Thomson and T.R.S. Wilson

I.O.S. Report No. 174

1983

*Present address:
Department of Earth Sciences
The University
Leeds, LS2 9JT
England

DEPARTMENT OF THE ENVIRONMENT

RADIOACTIVE WASTE MANAGEMENT

RESEARCH PROGRAMME 1983/84

DoE Report No. DoE/RW/ 83/146

Contract Title: The properties of ocean sediments in relation to the disposal of radioactive waste

DoE Reference: DGR 481/177

Report Title: Geochemistry of the near surface sediments of the Nares Abyssal Plain

Author s CARPENTER, M.S.N. et al

Date of submission to DoE 22.2.1983

Period covered by report

Abstract

The geochemistry of a suite of box and 2m gravity cores from the Nares Abyssal Plain has been characterised by means of pore water analyses, XRF determination of major and trace element concentrations, mineralogy and $^{230}Th_{excess}$ dating. The interstitial fluid environment of those deep-sea clays is mildly reducing, although one site exhibits manganese remobilisation and precipitation. Despite their marked colour differences, there is a similarity in clay mineralogy between the grey silt/clay turbidites and the brown clays found in the area. Sediment accumulation rates of pelagic brown clays range between 0.5 and 1.0 cm/10^3yr. These pelagic brown clays are metal-rich relative to the grey clays, and a model is used to estimate the hydrogenous metal fluxes on the assumption that they are constant over the Plain. This model gives values of $\sim$1300 µg/cm^2/10^3yr for Mn, $\sim$2600 µg/cm^2/10^3 yr for Fe and Co, Ni, Cu, V and Zn in the range 6-26 µg/cm^2/10^3yr. An associated model-derived estimate of the detrital contents of the same elements agrees well with the mean values of the grey clays and of average shale. Metal-poor brown clays and assorted minor lithologies are intermediate in composition between these two end-members.

Keywords 94, 112,115,131,225
299

CONTENTS

1. INTRODUCTION

One of the most general observations that has been made concerning the geochemistry of deep-sea sediments is that they are enriched in a wide range of elements relative to their near-shore counterparts (e.g. WEDEPOHL, 1960; TUREKIAN and IMBRIE, 1966; CHESTER and MESSIHA-HANNA, 1970). Whilst it is now recognised that the consequences of hydrothermal activity are responsible for metal enrichment in the sediments surrounding areas of hydrothermal circulation on mid-ocean ridges (BOSTROM and PETERSON, 1969; EDMOND et al., 1979a, 1979b), the widespread occurrence of metal enriched sediments in the deep ocean is still poorly understood. The models proposed for such sediments (WEDEPOHL, 1960; TUREKIAN, 1967) have tended to emphasise the addition of a metal-rich hydrogenous (authigenic) component derived from seawater or originating as riverborne colloids to a lithogenous (detrital) component poor in metals and derived from continental weathering. There is surprising little information available, however, on the rates at which metals accumulate in deep sea sediments (KRISHNASWAMI, 1976; BACON and ROSHOLT, 1982) which is crucial for the testing of such models. This information is further important for assessing assumptions of chemical steady-state in the oceans by comparison of metal removal rates to sediments with input rates from rivers and hydrothermal activity.

The measurement of metal accumulation rates in pelagic sediments is now of particular relevance because of the interest in chemical fluxes within the oceans that has been generated by modelling of high-quality trace metal data for seawater (e.g. BRULAND, 1980; BOYLE et al., 1981) and from the direct estimation of particulate fluxes using sediment traps (e.g. BISHOP et al., 1977; SPENCER et al., 1978; HONJO, 1980; BALISTRIERI et al., 1981). In this paper we describe the results of a study of the geochemistry of deep-sea sediments of the Nares Abyssal Plain, N.W. Atlantic Ocean, an area where both slowly-accumulating pelagic sediments and rapid turbidite deposition is found. After distinguishing these sediment types and commenting on their geochemical and mineralogical characteristics, we present data on the accumulation rates of metals in the slowly-accumulating deposits and provide a model which partitions the metals between hydrogenous and detrital components, allowing us to comment on the variability of metal fluxes in deep ocean sediments.

2. REGIONAL SETTING

The Nares Abyssal Plain (Figure 1) is some 800 km long and 200-400 km wide, elongated east to west. On the large scale, our understanding of the sediment distribution found on the Plain derives mainly from complementary geophysical and piston core investigations (SHIPLEY, 1975, 1978; KELLER and LAMBERT, 1979; TUCHOLKE, 1980), both in the area of the Plain itself and its environs. Cores taken in the Plain commonly reveal stratified or laminated sediment sequences comprised of two main types of silty clay, a red or brown variety interpreted as pelagic, and a coarser grey variety interpreted as distal turbidites (SHIPLEY, 1978). The silty grey clays are found deposited only at water depths greater than 5670m. On the basis of the similarity of mineralogy, SHIPLEY (1978) has suggested that the grey and brown clays have the same ultimate origin, but are deposited from distal turbidity currents and the bottom nepheloid layer respectively. According to TUCHOLKE (1980) the Vema Gap at 5600-5800m provides the only major passage into the Nares Abyssal Plain for distal turbidity currents arising in the Hatteras Abyssal Plain. Thus the silt beds are observed to be thickest at the western end of the Nares Abyssal Plain and become thinner, although more numerous, to the east. These sediment transport processes nevertheless appear to persist into the two major fracture zone valleys at the north-east of the Plain, the Nares (sometimes Kane) Fracture Valley and the Nares Deep Fracture Valley. The Plain and these two valleys are interconnected by a large number of gaps in an abyssal hill topography. In this area the abyssal hills tend to be draped by brown clay rich in manganese nodules (ADDY 1979), while the grey clays, devoid of nodules, are found in the fracture valleys and interconnecting gaps (SHIPLEY, 1978, TUCHOLKE, 1980).

While there is now a reasonable geophysical data base for Nares Abyssal Plain sediments, there is less geochemical information. CHESTER et al., (1973) drew attention to the fact that the elements Mn, Ni and Co were enriched in some (but not all) upper sediments in the south-west area of the North Atlantic relative to a North Atlantic clay average. It was concluded that the enrichments approximated the composition of manganese nodules, and probably were derived from seawater. ADDY (1979) examined the rare earth element (REE) contents and patterns of nodules and micronodules from the abyssal hills in the area of the Nares Fracture and Deep Fracture Valleys. From the REE systematics he concluded that these elements in the nodules probably had a seawater origin, although the situation was more complex as regards micronodules. Differences were also found

in the contents of Mn, Fe, Ni, Co and Cu of nodules and micronodules co-existing in the same cores (ADDY, 1978). ADDY (1979) also demonstrated that the red clays which contained micronodules and nodules were enriched in REE, Mn, Fe, Ni and Co relative to the grey clays which had a low ferromanganese phase content.

Similarly, little pore-water data has been published for this region. ADDY, PRESLEY and EWING (1976) report dissolved and solid phase manganese profiles for a single, oxidising site on the north wall of the Puerto Rico trench. They conclude that the observed distributions at this site are due to post-depositional diagenetic remobilisation of a labile, hydrogenous fraction of the manganese at depths greater than 2 metres. SAYLES (1979) gives major element data for stations further south, but does not include data on redox-sensitive species. The present paper, therefore, presents the first detailed report on the redox status of the interstitial waters of the Nares Abyssal Plain and in the light of this information discusses the depositional and post-depositional histories of the sediments of this area.

3. METHODS

3.1 Sampling

Figure 1 illustrates the stations on a representation of the Nares Abyssal Plain and environs. Sediment sampling was performed with an I.O.S. box corer (PETERS et al., 1980) to retrieve the surface sediments, and with a Kastenlot gravity corer with 2m x 15cm square barrel to achieve greater depth. Confirmation of SHIPLEY's (1978) observation that grey turbidites are found only in water depths greater than 5700m is clearly illustrated in Table 1 which lists the details of the cores collected.

On deck, cores were processed as rapidly as possible. Solid phase samples were taken at 1 or 2cm sections at a spacing not greater than 5cm, and the sediment subsamples returned to the laboratory frozen at -18°C. Pore water samples were extracted from box and Kastenlot subcores taken by insertion of plastic tubes. The subcores were extruded into a nitrogen-filled glovebox, sectioned, and loaded into squeezers (RIDOUT, 1981). These were sealed and transferred to a cool (2°C) squeezing cabinet: after temperature equilibration pore water was expressed from the samples either by hydraulic hand-pump pressure or by nitrogen gas pressure. Samples were stored at 2°C until analysis.

3.2 Interstitial water analysis

Shipboard analysis was carried out for silicate and phosphate, using modifications of the methods described by STRICKLAND and PARSONS (1968). Accuracy is estimated at ±2% for silicate and ±5% for phosphate. Sample aliquots were returned to shore laboratories for the determination of manganese, nitrate, iodate and iodide. Iodate was measured by the method of TRUESDALE and SMITH (1979) and total iodine by the method of TRUESDALE (1978). Iodide was thus found by difference. Precision for iodine is estimated at ±1.2% and for iodate at ±4.3%. Nitrate was measured by a modification of the method of DAVISON and WOLF (1978, 1979) requiring 2.5ml of sample: precision is estimated at ±3%. Manganese was determined by flameless atomic absorption analysis, using a Perkin-Elmer type 360 A.A.S. fitted with a type 74 atomiser, giving a precision of 8.7% (McARTHUR, 1977).

The data obtained are tabulated as Appendix 1.

3.3 Sediment mineralogy and analysis

Samples were prepared as powders for analysis by drying at 110°C followed by grinding in agate. Mineralogical analyses were performed by XRD scans of random aggregate powder mounts on a Philips PW 1050 goniometer with a Cu-target tube. Quartz and clay mineral abundances were estimated by comparison with doped mixtures (α-alumina and quartz) and with pure clay mineral standards.

XRF analyses for major, minor and trace element contents were made with a Philips 1410 Spectrometer modified for automatic angle stepping and on-line data processing. Major element analyses were performed on glass discs, manufactured from fusion mixtures according to the methods of NORRISH and HUTTON (1969) and HARVEY et al., (1973) using a Cr-target tube. All samples were calcined at 1000°C before fusion in order to obtain gravimetric loss on ignition (L.O.I.) data and ensure an accurate flux:sample ratio (5.33 ± 0.02 : 1). Overall analytical precision is around 3% or less except for MnO and P_2O_5 (5%). Trace elements, sodium and chlorine were determined on pressed powder pellets composed of 6-9g of sediment with 0.5% wax binder. Na and Cl contents are precise to only 10% and 5% respectively. A W-target tube was used for trace element analyses: precision is 2-4% for most elements except Co (6%) and Nb and Cu (6-9%). No matrix correction was applied due to the presence of a heavy absorber in the flux.

Carbonate content and organic carbon contents were determined by gasometric analysis following LECO induction furnace and acid decomposition treatments. $CaCO_3$ content data is precise to about 5%, whereas the organic carbon data (obtained by difference) is precise to only about 10%.

The data obtained are tabulated as Appendix 2.

3.4 Radiochemical analysis

Analyses for the alpha-emitting isotopes were performed by a method described elsewhere (THOMSON, 1982). Briefly, 1-2g samples are spiked with $^{228}Th/^{232}U$ tracer, then completely dissolved after potassium fluoride and sodium/potassium pyrosulphate fusions. Uranium and thorium fractions are separated by ion exchange, and electroplated as sources for alpha spectrometry.

The data obtained are tabulated as Appendix 3.

4. RESULTS AND DISCUSSION

4.1 Interstitial waters

In order to interpret the observed solid phase composition profiles, it is important to evaluate the extent of post-depositional mobilisation and migration. For many of the elements of interest this is a function of the redox potential of the sedimentary environment.

Porewater composition analyses indicate that the sediments ampled are intermediate in redox status between the most oxidising sediments (e.g. GRUNDMANIS and MURRAY, 1982) at which no reduction is observed, and the much more intensely reducing conditions typical of equatorial and other areas of high productivity (e.g. FROELICH et al., 1979). In particular, the low levels of dissolved manganese observed (except in core 10164#1K), indicate that active diagenetic remobilisation of this element is not proceeding at present in most of the intervals sampled. From this, it is possible to conclude that the wide variations in manganese content of the solid phase originate either from depositional variations, or from periods of more intense reduction in the past. The latter hypothesis is unlikely. In order to produce the observed profiles, the sediment column would need to have become almost totally anoxic at some time within the last 100,000 years or so. All manganese peaks would then be generated as diagenetic relicts of previous shallow 'stands' of the redox boundary as it migrated downwards towards its presently observed position. It is difficult to visualise such a very strongly reducing profile in this abyssal plain environment. Consequently, it is concluded that the solid phase manganese distribution is predominantly depositional in origin at these sites: exceptions to this are found within the 30-40cm depth interval in core 10164#1K and 140-170cm interval in core 10163#1K (Figure 3). In both these intervals, high solid phase manganese values are measured close to the depth at which manganese begins to increase in the pore waters, and these two features are therefore probably diagenetic.

The iodide/iodate couple is an indicator of the redox state of pore waters. Reduction is calculated to take place over the narrow range pE = 10 to 10.7, which means that the couple indicates the depth at which this pE occurs very precisely, though the system is useful over a very limited dynamic range (WONG and BREWER, 1977). For this reason it would be expected that reduction would take place over a very restricted depth interval (e.g., Core 1064#1K, Fig.2). This behaviour is in fact observed at stations 10164 and 10165, but a more complex pattern is shown at stations 10163 and 10170 (see Fig. 2), and it seems possible

that these cores are poised at a rather higher pE value than the range indicated above, and further that a strong redox gradient is absent at both these stations. The normally accepted pattern of organic diagenesis in slowly accumulating sediments yields concentration profiles in a characteristic sequence and with a characteristic shape. Because the most intense diagenetic activity is found at the sediment-water interface, the slopes of the concentration profiles are normally greatest near this interface; conversely, slopes approach zero as depth in the sediment increases (FROELICH et al., 1979). This simple conceptual model, although consonant with the broad majority of the observations, is inadequate to explain certain features observed in our pore water profiles. For instance, in core 10164#1K the slopes of the silicate, manganese, total iodine and alkalinity profiles do not approach zero with increasing depth but tend to constant positive values: cf. Figure 2, which compares this core with the more typical 10163 profiles. These observations cannot be reconciled with a simple diagenetic model based on the concept of a constant, slow sedimentary accumulation. Instead, it is necessary to postulate that a relatively recent catastrophic event may have occurred at this site. If such an event had resulted in the burial of organic-rich material at or below 2 metres depth, then profiles of the observed shape could be generated.

In order to test this hypothesis, the fluxes implied by the observed gradients were calculated for the four species mentioned (Table 2). Assuming simple one-dimensional diffusion, the minimum time to approximate a steady-state linear profile is given by $Dt/1^2 = 0.45$ (CRANK, 1956). This gives minimum diffusion times on the order of 400 years for manganese (II) and 140 years for iodine. As the calculated fluxes given in Table 2 are quite small relative to the total quantities of material present, the linear gradients could thereafter be maintained for considerable periods by mobilising the solid phase. For instance, the dissolved manganese gradient of core 1016#1K could be maintained by the mobilisation of a quantity of solid phase manganese equivalent to the content of a 3cm thick layer of sediment every thousand years.

Similar conclusions can be drawn for other diffusing species in this core. It is thus clear that the pore water profiles at this site support the hypothesis that sedimentation has been sporadic and catastrophic, rather than continuous and gentle. Similar, but less dramatic, episodes may have occurred in some sections of other cores sampled. These conclusions are in agreement with the ^{230}Th data (see Section 4.2).

4.2 Sediment accumulation rates and $^{230}Th_{excess}$ data.

It has been remarked by SHIPLEY (1978) and KELLER and LAMBERT (1979) that there is a paucity of sediment accumulation rate data for the Nares Abyssal Plain, and in this study radiometric data for the $^{230}Th_{excess}$ method were gathered in parallel with the elemental data for this suite of cores. This method is based on the phenomenon of constant production of ^{230}Th by decay of ^{234}U in the water column, and its subsequent rapid removal and incorporation into the sediments. The customary procedure is to estimate a mean accumulation rate for the sediment column by measuring the decay of unsupported ^{230}Th ($^{230}Th_{excess}$) with depth (KU, 1976; GOLDBERG and BRULAND, 1974). By convention $^{230}Th_{excess}$ equals the total ^{230}Th specific activity measured minus the corresponding ^{234}U specific activity. If the rate of sediment accumulation has been constant in time, then:

$$\ln A = \ln A_o - \lambda . z/S$$

where A is the $^{230}Th_{excess}$ specific activity at depth z, A_o is the sediment interface value of $^{230}Th_{excess}$, λ is the decay constant for ^{230}Th and s is the sediment accumulation rate. Figure 3 illustrates plots of the data from the four box cores treated in this fashion, with mean sediment accumulation rates obtained from the slopes of the best-fit lines. (No rate can be estimated for core 10165#2BX because grey clay with low $^{230}Th_{excess}$ values is observed below 20cm, and this core will be discussed later along with the Kasten cores. Although a thin lens of grey clay is also observed in core 10163#3BX, a regression line has been drawn in this case because the influence on the full core section is minor.) For core 10164#5BX, $^{231}Pa_{excess}$ data are available (Appendix 2). These may be treated similarly to $^{230}Th_{excess}$ data and yield an independent (if less accurate because of lower activity level) estimate of accumulation of 0.42cm/10^3 yr which compares with the value of 0.49cm/10^3 yr from the $^{230}Th_{excess}$ method.

The process of bioturbation is commonly observed in the uppermost few centimeters of sediment in deep sea deposits (TUREKIAN et al., 1978), even in some slowly accumulating clays (COCHRAN and KRISHNASWAMI, 1980). This feature is not observed within the resolution of the data here and has been ignored in the calculation of mean rates. These three box cores yielding sedimentation rates are interpreted as having been formed under pelagic conditions, and are referred to subsequently as slowly accumulated brown clay.

It should be noted that the accumulation rates obtained (0.49 - 1.02 cm/10^3 yr) are higher than those estimated by SHIPLEY (1978) for the brown clay in this area since mid-Cretaceous time (0.1 - 0.3 cm/10^3 yr). They translate however to

clay fluxes of 0.3 - 0.7g/cm^2/10^3 yr, which are not unusually high values for Atlantic sediments in the past 100,000 years (TUREKIAN, 1965; BACON 1983). SHIPLEY (1978) observed that brown clay always overlay the uppermost grey unit in the cores he studied, and used his long-term accumulation rates to estimate that turbidity current activity (as revealed by the presence of grey clay units) had not been active for 300,000 years in the area. If the higher recent accumulation rates determined here are also applicable to the abyssal hills in the area of the Fracture Valleys where most of his cores were taken, they suggest that 300,000 years will be an overestimate. Specifically, a grey silt layer is found within 12cm of the surface in core 10163#3BX, a depth corresponding to an age of only 15,000 years.

$^{230}Th_{excess}$ data obtained for the two Kasten cores are illustrated in Figure 4. The section 29-71cm in core 10163#6K yields a rate of 0.51cm/10^3 yr and like the three box cores above is interpreted as slowly accumulated brown clay. Nevertheless, as with the case of box core 10165#2BX, no plausible sedimentation rate can be derived for most of the Kasten core sections because low and erratic $^{230}Th_{excess}$ values are observed. The $^{230}Th_{excess}$ method has little power when lateral movement and consequent sediment mixing has occurred. First, low $^{230}Th_{excess}$ values are expected when a sediment section moves, is mixed and redeposited; and second, rapidly accumulated sediment from shallower water will have low $^{230}Th_{excess}$ levels even before it is moved and introduced to greater depth. The interpretation of the grey clay units as turbidites leads to an expectation of low specific activities, and this is in accord with observation in the sections 150-200cm in core 10163#6K and 50-160cm in core 10164#1K.

A further useful aspect of $^{230}Th_{excess}$ data is that a comparison may be made of the sediment inventory of $^{230}Th_{excess}$ activity with that anticipated by supply from the overlying water column. ^{230}Th has one of the shortest water residence times known (BACON and ANDERSON, 1982) and the consensus opinion is that it does not tend to move out of the ocean basin in which it is formed (BACON and ROSHOLT, 1982). In view of calculations made later in this paper to estimate the fluxes of various elements removed from the water column to the sediments (Section 4.4), it is of interest to make this sediment/water column comparison for $^{230}Th_{excess}$. The comparison is in Table 3, where the water column supply is calculated from the uranium content and $^{234}U/^{238}U$ activity ratio of sea water (3.3 μg/ℓ and 1.14 respectively, KU et al., 1977) and the sediment column inventory evaluated from the expression (KRISHNASWAMI et al., 1971):

$$\Sigma = \frac{\rho.s.A_o}{\lambda}$$

where Σ is the $^{230}Th_{excess}$ inventory per cm^2, ρ is the *in situ* dry sediment density (measured for the slowly accumulated brown clay as $0.65 g/cm^3$), s is the mean sediment accumulation rate, A_o is the interface (regression line intercept) $^{230}Th_{excess}$ specific activity and λ is the ^{230}Th decay constant. It is evident from Table 3 that there is marked shortfall, around 40%, in the sediment inventory. KADKO (1980) found a deficit of 28% for 28 cores from the literature taken in water depths, between 4600 and 5800m, but attributed at least part of this to the effects of surficial sediment mixing on his model calculations. The reasons for the shortfall here are unclear, but the consistency for all three box cores suggest that the sediments are systematically failing to record the $^{230}Th_{excess}$ production of the full water column depth.

4.3 Geochemical and mineralogical characterization

This discussion is based on 62 sediment subsamples taken from four box cores and two Kastenlot cores obtained on four stations. Alternate layers of grey and reddish-brown clay were described in all cores taken at water depths greater than 5700m (Table 1), the grey clays generally forming graded silty units 10-80cm thick with coarse, sharp bases. The cores lacking grey silty interbeds were taken at shallower water depth; on a small topographic high (core 10164#5BX : 55cm homogenous brown clay in 5613m) and above the carbonate compensation depth on the northern flank of the Puerto Rico Trench outer ridge (core 10170#1BX ; 60cm of yellowish grey marls and brown clay in 5520m).

These observations are in agreement with those of SHIPLEY (1978), who concluded that the brown and grey clays are ultimately derived from the same source but that the grey clays represent distal turbidites (containing more silt-sized material) and the brown clays represent slow pelagic deposition. In this study, the following classification of sediment types has been adopted as a result of both core description and analytical data:-

1. Homogenous brown clays, subdivided into:
   (a) metal-rich or slowly accumulated brown clays,
   (b) metal-poor brown clays.
2. Grey clays with some silt-sized material.
3. Assorted minor lithologies, predominantly laminated and mottled clays and predominantly red/brown/orange in colour.

The first two major lithologies mentioned above account for 46 out of a total of 62 analyses, whereas minor lithologies such as orange and tan clays, laminated clays and yellowish marls, account for 16 analyses. Although the grey clays (18 analyses) are very heterogenous as a group (see Table 4), this variability is coherent in the sense that it can be explained in terms of co-variance of well correlated variables (see Table 5). The minor lithologies are included in the overall mean of Table 4 even though, as a group, they lack both chemical homogeneity and statistical coherence.

It is only in conjunction with $^{230}Th_{excess}$ data (see Section 4.2) that it is possible to subdivide the homogenous brown clays (28 analyses) into 1(a), slowly accumulated brown clays (16 analyses) with clear enrichment in metals generally regarded (e.g. reviews by CHESTER and ASTON, 1976; MURRAY and BREWER, 1977) as hydrogenous (Mn, Cu, Ni and Co) and 1(b) brown clays (12 analyses) with little or no enrichment in hydrogenous metals, i.e., metal-poor deep sea clays with no

evidence for slow, pelagic deposition (< 1cm/10^3 yr) yet exhibiting no evidence of turbidite characteristics.

In general, the variations in mineralogy between brown and grey clays support the suggestion of SHIPLEY (1978) that colour differences are not reflected in a primary way in mineralogy. XRD mineralogical scans on the same samples used for XRF analysis have revealed a marked but variable enrichment of calcite and quartz contents in the grey clays (up to 9% calcite and 15% quartz contents) compared with homogenous brown clays (< 2% calcite and < 8% quartz). Nevertheless, there appears to be little systematic difference in clay mineralogy between the brown and grey layers, as observed by ADDY (1978) and SHIPLEY (1978).

The major significant differences between slowly accumulated brown clays, metal-poor brown clays and grey clays are best summarized by correlation matrices for each group which identify the main controls on co-variance amongst the major and trace element data base (see Table 5). Chemical variation between groups can then be accounted for by changes in the relative importance of five cluster groups which are as follows:-

i) Ni, Co, Cu and MnO - micronodules are evident in the samples exhibiting this association; (both slowly accumulated and metal-poor brown clays).

ii) Al_2O_3, Zn, V and Fe_2O_3T - these elements are partly related to the Fe-rich hydrogenous component in slowly accumulated brown clays, and partly associated with impurities in kaolinite and/or chlorite in grey clays. They are excluded from the carbonate phase, and from metal-poor clays.

iii) K_2O, Rb and Cr - these elements are associated with illite (the dominant clay mineral phase in all groups). Cr may be associated with illite and chlorite in grey clays, but is excluded from illite in slowly accumulated brown clays.

iv) Sr, CO_2, organic C and CaO - here the association is with biogenic calcite, found mainly in grey clays.

v) SiO_2, Zr and Nb - these elements are associated with the quartz variation in grey clays.

These five groups of well correlated elements have been interpreted (see Table 5) in terms of mineralogical control, i.e. good positive correlations between pairs of elements are taken to imply a process such as solid solution or an association due to inclusions or coatings, whereas negative correlations imply an exclusion or dilution effect. If the major and trace element data base

were re-calculated on a salt-free, carbonate-free basis, the conclusions drawn from correlation matrices would no longer be valid, due to the removal of a major source of variance ($CaCO_3$) and the discrimination between slowly accumulated brown clays and grey clays would become statistically significant (at the 1σ level) only for organic carbon, Rb and the hydrogenous metals, Mn, Ni, Cu and Co.

In comparing the metal-rich brown clays (type 1(a)) with the grey clays (Table 4), it is apparent that the metal-poor homogenous brown clays and the assorted minor lithologies are intermediate in composition between the two 'end members' (pelagic clays and turbidites) in most respects apart from carbonate content. This overall enrichment in preserved biogenic calcite in grey clays is consistent with an initial rapid deposition and burial of biogenic material and subsequent transportation from shallower water sites to the Nares Abyssal Plain by turbidity currents. A comparison of the group mean compositions in Table 4 shows that slowly accumulated brown clays differ from metal-poor brown clays in having generally higher average contents of MnO, Ni, Cu and Co, but significantly lower contents of K_2O, Rb and Cr. These differences can be explained if the metal-poor brown clays result from either an "in situ" mixing of compositionally distinct end-members (i.e., pelagic clays and turbidites) or a chemical fractionation related to transport and settling of particles during a waning current regime. The latter hypothesis is supported by the grain size and mineralogical variation from grey silty clays through laminated clays to homogenous brown clays, which is observed in vertical succession in certain cores (10163#6K and 10164#1K).

The average grey clay composition as presented in Table 4 bears certain similarities to an average shale composition (WEDEPOHL, 1968) which is itself representative of near-shore type sediments. However, the SiO_2/Al_2O_3 ratio is much lower in the grey clays here (2.96) than Wedepohl's average shale (3.52) and there appears to be some enrichment in $Fe_2O_{3_T}$, MgO, TiO_2, Co, V and Zn, even when account is made for quartz dilution. It must be stressed that the grey clays are very heterogenous as a group and that their range of variation (apart from SiO_2, MgO, Rb, Sr, Y, V and Zn) encompasses average shale composition. The average mineral composition of shales (WEDEPOHL, 1971) shows much more quartz and feldspar than any Nares grey clays (see Table 6), whilst the proportion of kaolinite is much greater in all the Nares sediments than average shale and also most N. Atlantic sediments (GRIFFIN et al., 1968; WINDOM, 1976).

Since the metal-poor brown clays are intermediate in composition between

slowly accumulated brown clays and grey clays, we can assume that they probably result from intermediate and limited up-take of hydrogenous metals onto an illite dominated detrital matrix. This detrital assemblage shows evidence of grain size and mineral fractionation away from rapidly accumulated grey clay - the coarsest fraction of the silty grey clays appears enriched in quartz and has a clay mineralogy dominated by illite and chlorite. An enhancement of kaolinite in the slowly accumulated brown clays (relative to average shale) reflects either the finest grained fraction of transported near-shore sediment, or alternatively may reflect a greater proportion of windborne dust derived from the N.E. Trade Winds (DELANY, et al., 1967). Under no condition, however, can the trace element abundance pattern of the N.E. Trades aeolian dust (CHESTER and JOHNSON, 1971) explain the hydrogenous element enrichment of the slowly accumulated brown clays in the Nares Abyssal Plain.

In conclusion, the slower the rate of sedimentation for a particular core section, the greater is the uptake of hydrogenous metals and the greater is the relative proportion of kaolinite in the bulk mineraology. Thus there is an association between fine grained kaolinite and micronodules in the more pelagic of the Nares Abyssal Plain brown clays. The rate of accumulation for the metal-poor brown clays must be slow enough to ensure almost complete decomposition of organic material within the sediment whilst being fast enough to limit the growth of micronodules and coatings rich in hydrogenous metals. The more rapidly deposited grey clays lack micronodules and are comparable in terms of chemical composition to near-shore sediments - thus the grey clays represent a sporadic, detrital input of sedimentation which can be mixed in variable proportions with a pelagic component to produce the sections observed.

4.4 A model for metal accumulation in the slowly-accumulated brown clay

As discussed in the previous section, a comparison of the metal contents of the sediments with the $^{230}Th_{excess}$ data suggests an association between the elements Mn, Co, Ni and Cu and $^{230}Th_{excess}$ levels in the homogenous brown clay sediment types. Where the $^{230}Th_{excess}$ specific activities are high in the pelagic brown clay sections (indicating slow accumulation rates), high concentrations of those elements are also found. The converse also holds, for example in core 10163#6K between 80 and 100cm, where the homogenous brown clay has low $^{230}Th_{excess}$ values, these transition element contents are not greatly enriched over shale values (Figures 3 and 5). The fact that low contents of the redox sensitive element manganese are observed in the pore waters of the box core sections with high metal contents is taken as evidence that diagenesis is not the primary cause of enrichment (Section 4.1). It has been remarked previously that $^{230}Th_{excess}$ is considered to be supplied to the sediment entirely by scavenging from the water column, so it appears reasonable to expect a similar source for the transition element enrichment. This expectation prompts examination of the fluxes of the transition elements in the four instances where the radiometric data yield reasonable accumulation rates, (29-71cm in 10163#6K, and the box cores 10163#3BX, 10164#5BX and 10170#1BX).

In figure 6 the metal data have been averaged over the same core section intervals for which $^{230}Th_{excess}$ mean accumulation rates have been estimated, and their mean fluxes plotted against the total accumulation fluxes for the same intervals. This procedure is similar to a model developed by TUREKIAN (1965) for the case where all or part of the trace element content of a sediment is added at a rate independent of the clay accumulation rate (in fact Turekian did not find any case to utilise this model but suggested that $^{230}Th_{excess}$ might approximate to it). Here it is used to evaluate the concept that the transition element content is a function of a constant hydrogenous flux superimposed on a variable detrital flux of constant composition:

$$\Sigma F = F_H + k.S$$

where ΣF is the total mean flux of the element, F_H is the hydrogenous flux of the element, S is the total mean sediment flux and k is the concentration of the element in the detrital phase. The regression line data in Figure 6 therefore allow evaluation of both the hydrogenous flux and of the detrital phase content (Table 7). These values are averages over the sampled area of the Nares Abyssal

Plain and over a period of around 100,000 years. The linearity of the plots supports the assumption that the composition of the hydrogenous flux is constant over the area. Secondary factors not taken into account are the differences in water column depth and the indications from the box cores that there is a deficit in the $^{230}Th_{excess}$ sediment inventories relative to water column supply (Section 4.2).

The approach taken above is similar in concept, though different in approach, to other work with a similar theme of a constant hydrogenous flux superimposed on a detrital matrix of constant composition. Among these are the "trace element veil" concept for the world ocean as described by WEDEPOHL (1960) and further developed and criticised by TUREKIAN (1965, 1967), the "constant flux model" developed for Pacific sediments by KRISHNASWAMI (1976) and the "constant water column supply model" of BACON and ROSHOLT (1982) invoked for a site on the Bermuda Rise. There appear to be few other estimates of hydrogenous flux deduced from sediments. It is clear from Table 7 that there is only a modest agreement between the magnitudes of the fluxes obtained and literature values. Nevertheless, there does appear to be a tendency for the fluxes to decrease in the order observed here, i.e. Fe > Mn > Cu > Ni > Co > Zn $\sim$ V.

Recent work on the trace element content of seawater with low-contamination analytical procedures have reduced estimates of the absolute concentrations of most of the elements just discussed. As a consequence of these more accurate data an improved understanding of the element water column relationships with the major nutrients phosphate and silica has been established (BRULAND, 1980, BOYLE et al., 1981). Copper exhibits additional complexities in behaviour due to deep water scavenging and a regeneration into bottom water from diagenesis at shallow depth in sediments (BOYLE et al., 1977, 1981). Manganese is believed to be scavenged from the dissolved to the particulate phase throughout the water column (KLINKHAMMER and BENDER, 1980, LANDING and BRULAND, 1980) and a similar behaviour has been proposed for cobalt (KNAUER et al., 1982). While the relative importance of these different water column geochemistries may well vary from area to area of the ocean and vary the magnitude of the different fluxes, it appears that these variations do not dramatically alter the sequence observed. It is also noteworthy that the hydrogenous flux values determined for the north-east Atlantic are higher than those obtained for the Pacific by KRISHNASWAMI (1976) from a widely-spaced selection of cores.

Following the suggestion of CHESTER et al., (1973) that sediment enrichments

in this area approximate to the composition of manganese nodules, a further comparison of the model-derived hydrogenous fluxes (Figure 6 and Table 7) can be made with authigenic ferromanganese phases (nodules and micronodules) from the area of the Nares Fracture Valleys (ADDY, 1979). Figure 7a illustrates the result of this comparison, using mean values obtained from ADDY's (1979) data. In order to display all the information simultaneously it has been necessary to normalise the data against average shale. The plot for the hydrogenous flux has as its fixed point the same Mn enrichment factor (around 200) as that of the two micronodules selected. It is evident that the plots for nodules, micronodules and the hydrogenous flux are generally of the same order of size and sequence except for Cu. A perfect agreement is not expected, as MOORE et al., (1981), for example, have demonstrated that the top and bottom of a single nodule and its co-existing sediment can all have markedly different relative enrichments of Fe, Mn and congeners. ADDY (1978) has also shown from a comparison of complementary nodules and micronodules that differences usually exist. The best agreement in Figure 7a is between the mean of two of ADDY's (1979) separated micronodule fractions which were selected because they show the same Mn/Fe ratio as the hydrogenous flux. This might be expected as the slowly accumulated brown clays, which were the dominant sediment type used in the model to derive the hydrogenous flux, do themselves contain micronodules. Thus the same pattern of relative enrichment over shale values is also evident in Figure 7a for the means of the slowly accumulated (or metal-rich) clay type (Table 4).

The model also provides values for the detrital matrix on which the hydrogenous flux is superimposed. As can be seen from Table 7, these estimates are in close agreement with the mean grey clay composition listed in Table 4, except for manganese where diagenetic remobilisation is a known problem. This further supports the idea already discussed (Section 4.3) of a similar source, close in composition to average shale (WEDEPOHL, 1968), for both the brown clay and the grey clay types. The estimated detrital values also compare well with other data, from different methods, from the Bermuda Rise (BACON and ROSHOLT, 1982) and the North Atlantic (CHESTER and MESSIHA-HANNA, 1970). In Figure 7b the means of the slowly accumulated brown clay, the metal-poor brown clay and the grey clay (Table 4) are plotted on a similar basis to Figure 7a along with the model detrital matrix data. This illustrates the points just made concerning the similarity to average shale, and the effect of the superimposed hydrogenous flux on the two types of brown clay already identified in Section 4.3.

5. CONCLUSIONS

This investigation of six cores from five sites produces a more detailed appreciation of the geochemistry of the near surface (up to 2m) sediments of the Nares Abyssal Plain, as revealed by the sediment record and associated pore waters. Together with previous work it illustrates a complex geochemical situation apparently controlled by sedimentation processes.

In line with SHIPLEY's (1978) observations, grey silty clay turbidites were observed only in cores taken from water depths greater than 5700m. Despite the marked colour difference, comprehensive major element and mineralogical data here confirm the similarity noted by Shipley between those grey clays and the pelagic brown clay also commonly observed.

The major modifications introduced here to SHIPLEY's (1978) representation are that:

i) over a 10^5 year time scale the $^{230}Th_{excess}$ data indicate a higher rate of pelagic sediment accumulation than previously estimated, but consistent with other Atlantic clay accumulation values.

ii) a grey clay unit found within a decimetre or so of the surface in a box core from the eastern end of the Plain demonstrates that turbidity currents have been active until much more recently (on the order of 10^4 yrs) than shown by previous work (10^5 yrs).

and iii) besides the two types of sediment already referred to, there are other sediment types which have brown as the main colour but which do not appear to be pelagic.

Interstitial water analyses reveal that the pore water condition is very mildly reducing. In general mobilisation of the redox sensitive element manganese into pore solution is not observed in the top 0.5-1m, and this is interpreted as evidence that no diagenetic migration of elements in this zone is occurring. An exception was observed in one core (10164#1K), and here it has been possible to model the data on the assumption of relatively recent burial of organic material at depth. It is found that profiles similar to those found could have been established in only a few hundred years in these circumstances, and thereafter maintained as oxidation proceeded.

A strong association has been demonstrated in the brown clays between the $^{230}Th_{excess}$ data and the hydrogenous suite of elements. In those cases where the $^{230}Th_{excess}$ data are consistent with slow sediment accumulation, clear enrichments of Mn, Co, Ni and Cu, and less marked enrichments of V, Fe and Zn are

found. These enrichments are not found in the grey clay sections and are less in brown clays with low and erratic $^{230}Th_{excess}$ values. On the basis of this observation a model has been applied to the area of the Nares Abbysal Plain which allows estimation of the hydrogenous fluxes of these metals and of their detrital clay matrix concentrations. The values of the hydrogenous fluxes follow a pattern broadly similar to that found in previous studies, but it is clear that the absolute flux values exhibit considerable geographical variation. The detrital concentrations agree well with the means of the grey clay analyses and are close to shale values.

6. REFERENCES CITED

ADDY, S.K. (1978) Distribution of Fe, Mn, Cu, Ni and Co in coexisting manganese nodules and micronodules. Marine Geology, 28, M9-M17.

ADDY, S.K. (1979) Rare earth element patterns in manganese nodules and micronodules from northwest Atlantic. Geochimica et Cosmochimica Acta, 43, 1105-1115.

ADDY, S.K., B.J. PRESLEY and M. EWING (1976) Distribution of manganese, iron and other trace elements in a core from the northwest Atlantic. Journal of Sedimentary Petrology, 46, 813-818.

BACON, M.P. (1983) Glacial to interglacial changes in carbonate and clay sedimentation in the Atlantic estimated from Th-230 measurements. (Preprint of unpublished manuscript).

BACON, M.P. and R.F. ANDERSON (1982) Distribution of thorium isotopes between dissolved and particulate forms in the deep sea. Journal of Geophysical Research, 87, 2045-2056.

BACON, M.P. and J.N. ROSHOLT (1982) Accumulation rates of Th-230, Pa-231, and some transition metals on the Bermuda Rise. Geochimica et Cosmochimica Acta, 46, 651-666.

BALISTRIERI, L., P.G. BREWER and J.W. MURRAY (1981) Scavenging residence times of trace metals and surface chemistry of sinking particles in the deep ocean. Deep-Sea Research, 28A, 101-121.

BISHOP, J.K.B., J.M. EDMOND, D.R. KETTEN, M.P. BACON and W.B. SILKER (1977) The chemistry, biology, and vertical flux of particulate matter from the upper 400m of the equatorial Atlantic Ocean. Deep-Sea Research, 24, 511-548.

BOSTROM, K. and M.N.A. PETERSON (1969) The origin of aluminium-poor ferromanganoan sediments in areas of high heat flow on the East Pacific Rise. Marine Geology 7, 427-442.

BOYLE, E.A., S.S. HUESTED and S.P. JONES (1981) On the distribution of copper, nickel and cadmium in the surface waters of the North Atlantic and North Pacific Ocean. Journal of Oceanographic Research, 86, 8048-8066.

BOYLE, E.A., F.R. SCLATER and J.M. EDMOND (1977) The distribution of dissolved copper in the Pacific. Earth and Planetary Science Letters, 37, 38-54.

BRULAND, K.W. (1980) Oceanographic distributions of cadmium, zinc, nickel and copper in the north Pacific. Earth and Planetary Science Letters, 47, 176-198.

CHESTER, R. and R.G. MESSIHA-HANNA (1970) Trace element partition patterns in North Atlantic deep-sea sediments. Geochimica et Cosmochimica Acta 34, 1121-1128.

CHESTER, R. and L.R. JOHNSON (1971) Trace element geochemistry of North Atlantic aeolian dusts. Nature, 231, 176-178.

CHESTER, R. and S.R. ASTON (1976) The geochemistry of deep-sea sediments. In Chemical Oceanography 2nd Edition, Vol. 6. J.P. RILEY and R. CHESTER, editors, Academic Press, pp.281-390.

CHESTER, R., L.R. JOHNSON, R.G. MESSIHA-HANNA and R.C. PADGHAM (1973) Similarities between Mn, Ni and Co contents of deep-sea clays and manganese nodules from the south-west region of the North Atlantic. Marine Geology, 14, M15-M20.

COCHRAN, J.K. and S. KRISHNASWAMI (1980) Radium, thorium, uranium and ^{210}Pb in deep-sea sediments and sediment pore waters from the North Equatorial Pacific. American Journal of Science, 280, 849-889.

CRANK, J. (1956) The mathematics of diffusion. Clarendon Press, Oxford. 347pp.

DAVISON, W. and C. WOLF (1978) Comparison of different forms of cadmium as reducing agents for the batch determination of nitrate. Analyst, 103, 403-406.

DAVISON, W. and C. WOLF (1979) Interference studies in the batch determination of nitrate in freshwater by reduction with cadmium to nitrite. Analyst, 104, 385-390.

DELANY, A.C., A.C. DELANY, D.W. PARKIN, J.J. GRIFFIN, E.D. GOLDBERG and B.E.F. REIMANN (1967) Airborne dust collected at Barbados. Geochimica et Cosmochimica Acta, 31, 885-909.

EDMOND, J.M., C. MEASURES, R.E. McDUFF, L.H. CHAN, R. COLLIER, B. GRANT, L.I. GORDON and J.B. CORLISS (1979a) Ridge crest hydrothermal activity and the balances of the major and minor elements in the ocean: the Galapagos data. Earth and Planetary Science Letters, 46, 1-18.

EDMOND, J.M., C. MEASURES, B. MAGNUM, B. GRANT, F.R. SCLATER, R. COLLIER, A. HUDSON, L.I. GORDON and J.B. CORLISS (1979b) Earth and Planetary Science Letters, 46, 19-30.

FANNING, K.A. and M.E.Q. PILSON (1874) The diffusion of dissolved silica out of deep-sea sediments. Journal of Geophysical Research, 79, 1293-1297.

FROELICH, P.N., G.P. KLINKHAMMER, M.L. BENDER, N.A. LUEDKI, G.R. HEATH, D. CULLEN, P. DAUPHIN, D. HAMMOND and B. HARTMAN (1979) Early oxidation of organic matter in pelagic sediments of the Eastern Equatorial Atlantic: suboxic diagenesis. Geochimica et Cosmochimica Acta, 43, 1075-1090.

GLACCUM, R.A. (1978) The mineralogical and elemental composition of mineral aerosols over the North Atlantic: the influence of Saharan dust. Ph.D. Thesis, University of Miami, Miami, 160pp.

GOLDBERG, E.D. and K.W. BRULAND (1974) Radioactive geochronologies. In The Sea, Vol. 5. E.D. GOLDBERG, editor, John Wiley and Sons, pp.451-489.

GRIFFIN, J.J., H.L. WINDOM and E.D. GOLDBERG (1968) The distribution of clay minerals in the world ocean. Deep-Sea Research, 15, 433-459.

GRUNDMANIS, V. and J.W. MURRAY (1982) Aerobic respiration in pelagic marine sediments. Geochimica et Cosmochimica Acta, 46, 1101-1120.

HARVEY, P.K., D.M. TAYLOR, R.D. HENDRY and F. BANCROFT (1973) An accurate fusion method for the analysis of rocks and chemically related materials by X-ray fluorescence spectrometry. X-Ray Spectrometry, 2, 33-44.

HONJO, S. (1980) Material fluxes and modes of sedimentation in the mesopelagic and bathypelagic zones. Journal of Marine Research, 38, 53-97.

KADKO, D. (1980) ^{230}Th, ^{226}Ra and ^{222}Rn in abyssal sediments. Earth and Planetary Science Letters, 49, 360-380.

KELLER, G.H. and D.N. LAMBERT (1979) Variation of sediment geotechnical properties between the Greater Antilles Outer Ridge and the Nares Abyssal Plain. Marine Geotechnology, 4, 125-143.

KLINKHAMMER, G.P. and M.L. BENDER (1980) The distribution of manganese in the Pacific Ocean. Earth and Planetary Science Letters, 46, 361-384.

KNAUER, G.A., J.H. MARTIN and R.M. GORDON (1982) Cobalt in north-east Pacific waters. Nature, 297, 49-51.

KRISHNASWAMI, S. (1976) Authigenic transition elements in Pacific pelagic clays. Geochimica et Cosmochimica Acta, 40, 425-434.

KRISHNASWAMI, S., D. LAL, J.M. MARTIN and M. MAYBECK (1971) Geochronology of lake sediments. Earth and Planetary Science Letters, 11, 407-414.

KU, T.L. (1976) The uranium-series methods of age determination Annual Review of Earth and Planetary Sciences, 4, 347-379.

KU, T.-L., K.G. KNAUSS and G.G. MATHIEU (1977) Uranium in open ocean: concentration and isotopic composition. Deep-Sea Research, 24, 1005-1017.

LANDING, W.M. and K.W. BRULAND (1980) Manganese in the north Pacific. Earth and Planetary Science Letters, 49, 45-56.

McARTHUR, J.M. (1977) Manganese determination in natural waters by flameless atomic absorption spectrophotometry. Analytica Chimica Acta, 93, 77-83.

LI, Y.H. and S. GREGORY (1974) Diffusion of ions in sea water and in deep-sea sediments. Geochimica et Cosmochimica Acta, 38, 703-714.

MOORE, W.S., T.-L. KU, J.D. McDOUGALL, V.M. BURNS, R. BURNS, J. DYMOND, M.W. LYLE and D.Z. PIPER (1981) Fluxes of metals to a manganese nodule: radiochemical, chemical, structural and mineralogical studies. Earth and Planetary Science Letters, 52, 151-171.

MURRAY, J.W. and P.G. BREWER (1977) Mechanisms of removal of magnanese, iron and other trace metals from sea water. In Marine Manganese Deposits. G.P. GLASBY, editor, Elsevier, pp.291-325.

NORRISH, K. and J.T. HUTTON (1969) An accurate X-ray spectrographic method for the analysis of a wide range of geological samples. Geochimica et Cosmochimica Acta, 33, 431-453.

PETERS, R.D., N.T. TIMMINS, S.E. CALVERT and R.J. MORRIS (1980) The I.O.S. box corer: its design, development, operation and sampling. I.O.S. Report No.106. 7pp (unpublished manuscript).

RIDOUT, P.S. (1981) A ship-board system for extracting interstitial water from deep ocean sediments. I.O.S. Report No. 121. 13pp (unpublished manuscript).

SAYLES, F.L. (1979) The composition and diagenesis of interstitial solutions. 1. Fluxes across the seawater-sediment interface in the Atlantic Ocean. Geochimica et Cosmochimica Acta, 43, 527-545.

SHIPLEY, T.H. (1975) Echo characteristics, reflector horizons and geology of the western central North Atlantic. Ph.D. thesis, Rice University, Houston. 156p.

SHIPLEY, T.H. (1975) Sedimentation and echo characteristics in the abyssal hills of the west-central North Atlantic. Bulletin of the Geological Society of America, 89, 397-408.

SPENCER, D.W., P.G. BREWER, A. FLEER, S. HONJO, S. KRISHNASWAMI and Y. NOZAKI (1978) Chemical fluxes from a sediment trap experiment in the deep Sargasso Sea. Journal of Marine Research, 36, 493-523.

STRICKLAND, J.D.H. and T.R. PARSONS (1968) A Practical Handbook of Seawater Analysis. Fisheries Research Baord of Canada, Ottawa, 311pp.

THOMSON, J. (1982) A total dissolution method for determination of the α-emitting isotopes of uranium and thorium in deep-sea sediments. Analytica Chimica Acta, 142, 259-268.

TRUESDALE, V.W. (1978) The automatic determination of iodate and total iodine in seawater. Marine Chemistry, 6, 253-273.

TRUESDALE, V.W. and C.J. SMITH (1979) A comparative study of three methods for the determination of iodate in seawater. Marine Chemistry, 7, 133-139.

TUCHOLKE, B.E. (1980) Acoustic environment of the Hatteras and Nares Abyssal Plains, western North Atlantic Ocean, determined from velocities and physical properties of sediment cores. Journal of the Acoustical Society of America, 68, 1378-1390.

TUREKIAN, K.K. (1965) Some aspects of the geochemistry of marine sediments. In Chemical Oceanography Vol. 2. J.P. RILEY and G. SKIRROW, editors, Academic press, pp.81-126.

TUREKIAN, K.K. (1967) Estimates of the average Pacific deep-sea clay accumulation rate from material balance considerations. Progress in Oceanography, 4, 226-244.

TUREKIAN, K.K. and J. IMBRIE (1966) The distribution of trace elements in deep-sea sediments of the Atlantic Ocean. Earth and Planetary Science Letters, 1, 161-168.

TUREKIAN, K.K., J.K. COCHRAN and D.J. DEMASTER (1978) Bioturbation in deep-sea deposits: rates and consequences. Oceanus, 21, 34-41.

WEDEPOHL, K.H. (1960) Spurenanalytische Untersuchungen an Tiefseetonen aus dem Atlantik. Geochimica et Cosmochimica Acta, 18, 200-231.

WEDEPOHL, K.H. (1968) Chemical fractionation in the sedimentary environment. In Origin and distribution of the elements. L.H. AHRENS, editor, Pergamon Press, pp.999-1016.

WEDEPOHL, K.H. (1971) Environmental influences on the chemical composition of shales and clays. In Physics and chemistry of the Earth. Vol. 8 L.H. AHRENS, F. PRESS, S.K. RUNCORN and H.C. UREY, editors, Pergamon, pp.307-333.

WINDOM, H.L. (1976) Lithogenous material in marine sediments. In Chemical Oceanography 2nd Edition, Vol. 5, J.P. RILEY and R. CHESTER, editors, Academic Press, pp.103-135.

WONG, G.T.F. and P.G. BREWER (1977) The marine chemistry of iodine in anoxic basins. Geochimica et Cosmochimica Acta, 41, 151-159.

Table 1 Details of cores collected

Core	Type	Latitude (N)	Longitude (W)	Depth (Corr. m)	Percentage of grey clay
10163#3BX	Box	23°41.3'	59°40.9'	5933	31
10163#6K	Kasten	23°43.5'	59°41.7'	5947	20
10164#1K	Kasten	26°14.0'	60°20.7'	6221	62
10164#5BX	Box	26°04.9'	60°24.7'	5613	0
10165#2BX	Box	23°43.8'	61°29.4'	5900	40
10169#4K	Kasten	23°44.8'	65°13.0'	5835	91
10170#1BX	Box	21°43.6'	65°30.5'	5520	0

Table 2 Calculated diffusive fluxes in the interstitial waters of core 10164#1K.

	Manganese	Alkalinity	Total Iodine	Silicate
Concentration gradient (μmoles cm^{-4})	0.0016	.0025	3.6×10^{-6}	.0013
Effective diffusion coefficient (cm^2 sec^{-1})*	1.3×10^{-6}	3×10^{-6}	5.2×10^{-6}	3.3×10^{-6}
Flux (μmoles cm^{-2} sec^{-1})	2.1×10^{-9}	7.5×10^{-9}	1.9×10^{-11}	4.4×10^{-9}
Time to steady state (yrs)+	110	48	28	43

* Silicate value from FANNING and PILSON (1974). Other values from LI and GREGORY (1974). Assumed temperature 0°C and $\alpha\theta^{-2} = 0.55$.

\+ Minimum values as assumption is made that linear portion does not extend below sampled interval. Criterion for steady state $Dt\,\ell^{-2} > 0.45$ (CRANK, 1956).

Table 3 Comparison of $^{230}Th_{excess}$ water column production with sediment column inventory.

Core	Corrected Water Depth (m)	Steady state water column production (P d.p.m./cm²)	Calculated Sediment column inventory* (Σ d.p.m./cm²)	$\frac{\Sigma}{P}$
10163#3BX	5933	1600	940	0.59
10164#5BX	5613	1500	910	0.61
10170#1BX	5520	1500	1000	0.67

*Calculated with an in situ dry sediment density of 0.65 g/cm³ (measured).

Table 4 Average major and trace element composition of bulk sediment samples (this study) compared with average shale composition (WEDEPOHL, 1968).

	Nares Abyssal Plain sediments: overall mean of 62 Analyses	Slowly accumulated brown clays. Group mean N=16	Metal-poor brown clays Group mean N=12	Assorted minor Lithologies Group mean N=19	Grey clays Group Mean N=15	Average Shale Wedepohl (1968)
SiO_2	50.61 (2.25)	50.06 (0.57)	51.06 (1.39)	50.12 (2.35)	51.44 (3.38)	58.61
Al_2O_3	17.88 (1.12)	18.61 (0.72)	18.12 (0.74)	17.64 (0.98)	17.64 (1.44)	16.63
Fe_2O_{3T} ‡	7.85 (0.65)	8.15 (0.14)	8.14 (0.43)	7.83 (0.49)	7.35 (0.95)	6.89
MnO	0.35 (0.20)	0.53 (0.14)	0.29 (0.10	0.34 (0.17)	0.10* (0.04)	0.11
MgO	3.17 (0.26)	3.03 (0.13)	3.28 (0.25)	3.12 (0.26)	3.29 (0.28)	2.60
CaO	1.91 (1.59)	1.07 (0.28)	1.26 (0.37)	2.28 (2.26)	2.84 (1.36)	2.21
K_2O	3.55 (0.34)	3.33 (0.14)	3.66 (0.20)	3.57 (0.40	3.68 (0.42)	3.61
TiO_2	0.82 (0.22)	0.81	0.82	0.81	0.89	0.77
P_2O_5	0.17 (0.00)	0.17	0.18	0.17	-	0.16
NaCl	2.41 (0.38)	2.69	2.81	2.04	1.85	0.92
Na_2O	1.45 (0.17)	1.55	1.50	1.40	1.40	2.10
LOI ‡	9.33 (1.42)	9.22	8.64	9.48	9.79	
TOTAL	99.42 (2.13)	99.37	99.98	99.40	100.27	
CO_2	1.40 (1.10)	0.64 (0.40)	0.84 (0.40)	1.57	2.23 (1.20)	1.3
Org.C	0.27 (0.17)	0.17 (0.10)	0.16 (0.13)	0.28	0.42 (0.14)	
Rb	157 (13)	146 (3)	161 (6)	158 (14)	162 (17)	140
Sr	155 (19)	152 (12)	139 (14)	165 (64)	158 (35)	300
Y	31 (2)	32	30	32	31	41
Zr	135 (15)	130 (10)	135 (13)	133 (12)	142 (22)	160
Nb	17 (2)	17	18	17	17	18
Ni	78 (24)	107 (29)	79 (16)	69 (15)	56 (10)	68
Co	38 (17)	59 (13)	39 (14)	32 (10)	24 (4)	19
V	165 (12)	170 (9)	170 (7)	166 (8)	155 (17)	130
Cr	96 (6)	92 (3)	100 (3)	99 (5)	94 (8)	90
Cu	77 (15)	122 (20)	76 (2)	65 (22)	45 (20)	45
Zn	126 (9)	132 (4)	128 (4)	125 (7)	117 (12)	95

Nares samples are grouped into three main classes according to colour and inferred accumulation rate; N is total number of samples assigned to each group, and figures in brackets are standard deviations of the mean. * indicates 3 high values excluded from mean. Units: SiO_2 - Org C, % wt; Rb - Zn, ppm (dry basis). ‡ LOI - loss on ignition (1000°C).

‡ Fe_2O_{3T} - all Fe expressed as Fe(III).

Table 5 Summary of correlation coefficients calculated for pairs of chemical variables in overall database, slowly accumulated brown clays (1a) metal-poor brown clays (1b) and grey clays (2)

	Correlation Coefficients: Overall 62x27 matrix	(1a) 16x16 matrix	(1b) 12x12 matrix	(2) 15x15 matrix		Interpretation and Comments.
Ni Co	0.94	0.81	0.94	-	1	Controlled by variations in hydrogenous component: enriched in slowly accumulated brown clays, affected by Mn diagenesis.
Ni Cu	0.89	0.72	0.87	(0.23)		
Cu Co	0.87	0.72	0.72	-		
MnO Ni	(0.53)	0.93	(0.66)	(0.02)		
Ni Sr	(0.06)	0.72	0.89	(-0.37)		
MnO V	(0.41)	0.71	(-0.33)	(0.31)		
MnO Zn	(0.44)	0.67	(-0.04)	(0.31)		
Al_2O_3 V	0.88	0.84	-	0.95	2	Controlled by variations in kaolinite + associated impurities (Fe-rich): partly associated with hydrogenous component, partly associated with heterogenous grey clays.
Al_2O_3 Zn	0.88	0.82	-	0.96		
Zn V	0.86	0.86	(0.02)	0.96		
Fe_2O_3 Zn	0.85	(0.48)	(0.55)	0.93		
Fe_2O_3 Al_2O_3	0.83	(0.54)	-	0.92		
Fe_2O_3 V	0.82	0.69	(0.27)	0.93		
K_2O Rb	0.93	(0.29)	(0.52)	0.97	3a	Controlled by variations in illite: enriched in grey silty clays, excluded from slowly accumulated brown clays.
Rb Cr	(0.56)	(0.01)	(0.15)	0.94		
K_2O Cr	(0.53)	-0.67	(0.55)	0.93		
Al_2O_3 Cr	(0.35)	0.74	-	0.92	3b	Controlled by variations in impurities common to chlorite and kaolinite, mostly in grey clays.
Fe_2O_3 Cr	(0.55)	(0.18)	(0.52)	0.97		
Zn Cr	(0.40)	(0.47)	(0.22)	0.96		
CO_2 Sr	0.74	(0.27)	-	0.80	4	Controlled by variations in calcite in grey clays.
CaO CO_2	(0.44)	-	-	-		
CaO Org C	0.71	-	-	0.75*		
SiO_2 Zr	(0.54)	(0.1)	-	0.83	5	Controlled by variation in quartz and zircon content in grey clays.
Zr Nb	(0.55)	-	-	-		

Footnote: All positive, highly significant correlations are quoted from each separately established matrix. Values in brackets are only weakly significant ($r \leq 0.66$) and absent values are due to limitations in numbers of variables in each particular matrix.

* indicates r value from 20x20 matrix on station 10164 data alone.

Table 6 Mineralogical composition of Nares Abyssal Plain sediments (1) compared with composition of average shale (2) aeolian dust (3 and 4)and N. Atlantic deep-sea sediments (5)

	1	2	3	4	5
Illite	40-55	45-55	37	54	48
Quartz	<5-15	20	10	-	13
Feldspar	1-5	10-15	-	-	-
Chlorite	0-10	14	9	13	9
Kaolinite	15-30		29	28	17
Smectite	0-10	-	-	≤5	14
Calcite	0-10	3	14	-	-
$\frac{K+C^*}{I}$	0.28	0.6 - 1.2	1.0	0.76	0.54

Footnote: 1. Range of 62 bulk XRD scans (this study)

2. American and European shales (WEDEPOHL, 1971)

3. N.E. Trade wind dust, Barbados (DELANY, et al., 1967)

4. " " " " " (GLACCUM, 1978)

5. (GRIFFIN et al., 1968; WINDOM, 1976).

All values quoted as either average composition or total range of percent weight abundance

*K+C/I is ratio of kaolinite plus chlorite to illite.

Table 7 Comparison of estimated (i) pelagic brown clay detrital compositions and (ii) hydrogenous fluxes, of V, Mn, Fe, Co, Ni, Cu and Zn.

(i) Detrital compositions (p.p.m. by weight)

Element	Nares A.P. brown clay	Nares A.P. grey clay[a]	Bermuda Rise (GPC-5)[b]	North Atlantic average[c]	Pacific[d]	Average shale[e]
V	157±11	157	-	-	-	130
Mn	570±360	770	600±300	582	2087	850
Fe($\times 10^{-3}$)	49.2±1.2	51.8	51±3	-	38-43	48
Co	24 ±13	27	23±2	12	31-48	19
Ni	63 ±15	60	66±4	63	51-92	68
Cu	50 ±10	52	36±9	67	169-224	45
Zn	114 ±6	118	124±7	-	-	95

(ii) Hydrogenous fluxes ($\mu g/cm^2 . 10^3$ yr)

Element	Nares Abyssal Plain	Northwest Atlantic (Gulf Stream)[b]	Caribbean[f]	Pacific[d]
V	6±2	-	-	-
Mn	1300±50	4300±1100	-	500
Fe	2600±200	-	-	800
Co	13±2	7.2±5.7	7.4	5
Ni	17±2	46±16	10.7	10
Cu	26±2	76±26	19.2	8
Zn	7±1	17±20	-	-

a. Table X, this work.

b. BACON and ROSHOLT (1982)

c. CHESTER and MESSIHA-HANNA (1970)

d. KRISHNASWAMI (1976)

e. WEDEPOHL (1968)

f. TUREKIAN (1965)

Note: uncertainties quoted are derived from one standard deviation of the regression line slopes and intercepts.

Figure 1: A representation of the Nares Abyssal Plain and environs, showing coring stations and inferred turbidity current dispersal paths (after TUCHOLKE, 1980). (Reproduced by kind permissions of Dr. B.E. Tucholke and the American Institute of Physics.)

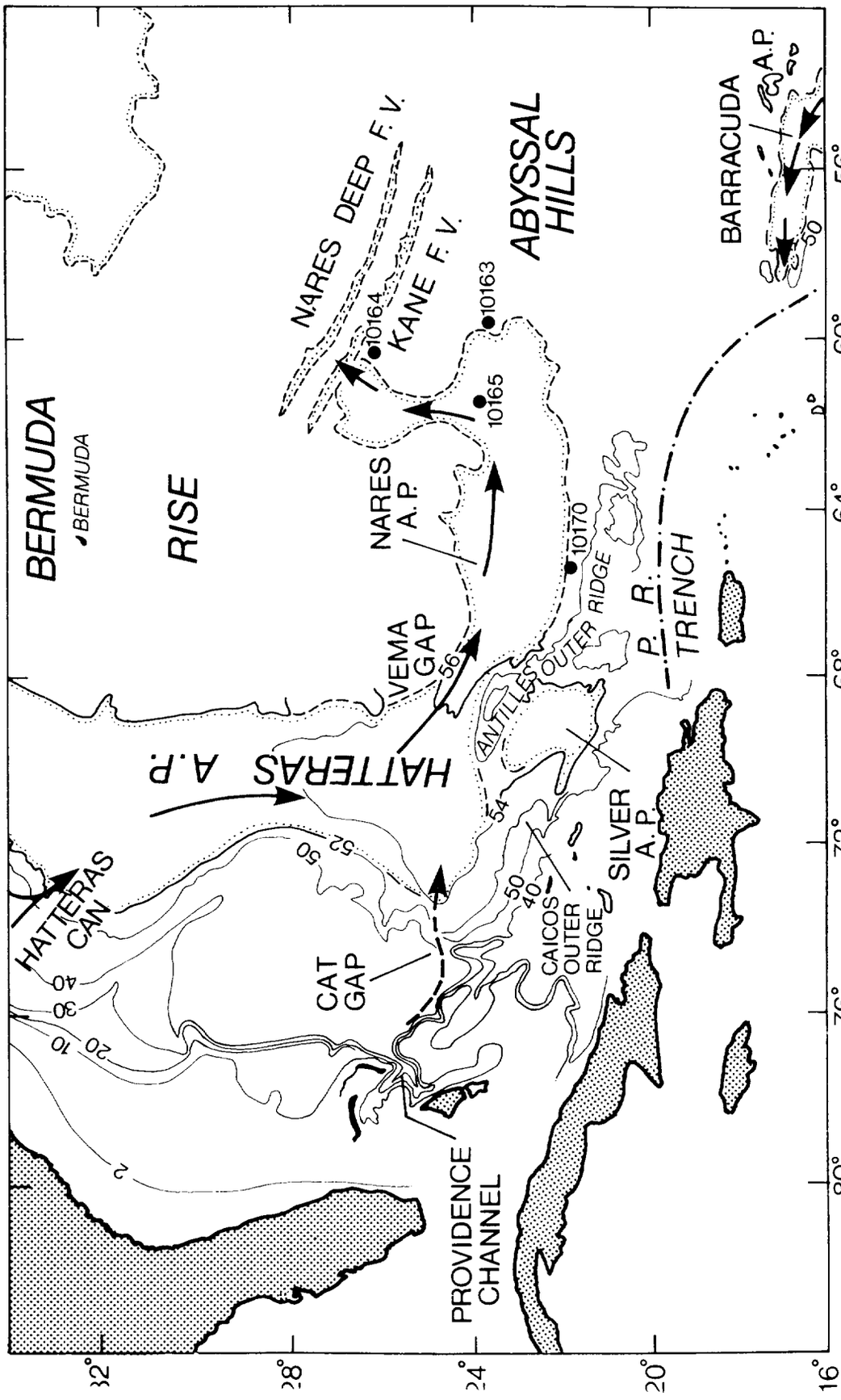
BERMUDA
BERMUDA
RISE
NARES DEEP F.V.
KANE F.V.
ABYSSAL HILLS
BARRACUDA
A.P.
10164
10163
10165
10170
NARES A.P.
VEMA GAP
HATTERAS A.P.
ANTILLES OUTER RIDGE
P. R. TRENCH
HATTERAS CAN
CAT GAP
CAICOS OUTER RIDGE
SILVER A.P.
PROVIDENCE CHANNEL
2
10
20
30
40
50
52
54
56
50
40
50
32°
28°
24°
20°
16°
80°
76°
72°
68°
64°
60°
56°

Figure 2: Concentration/depth profiles of the interstitial water contents of iodine, manganese and silica at Stations 10163 and 10164. The profiles are composites from both box and Kasten cores recovered at these stations.

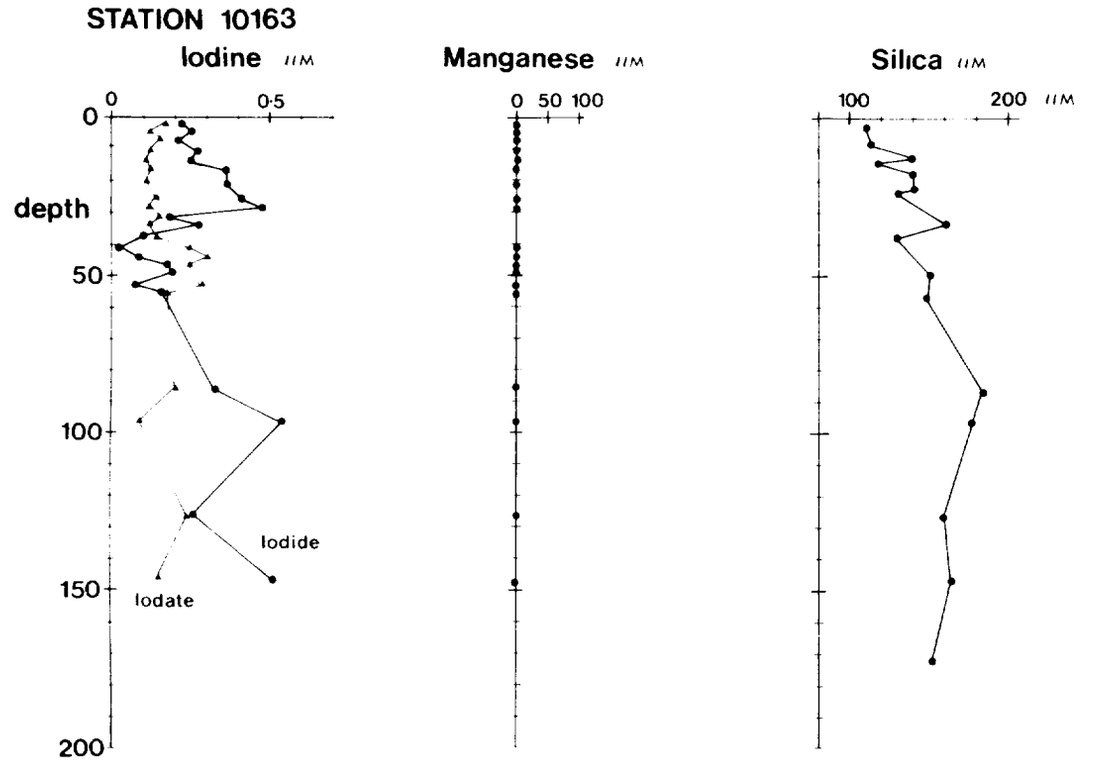
STATION 10163
Iodine µM
Manganese µM
Silica µM
0
0·5
0 50 100
100
200 µM
depth
0
50
100
150
200
Iodide
Iodate

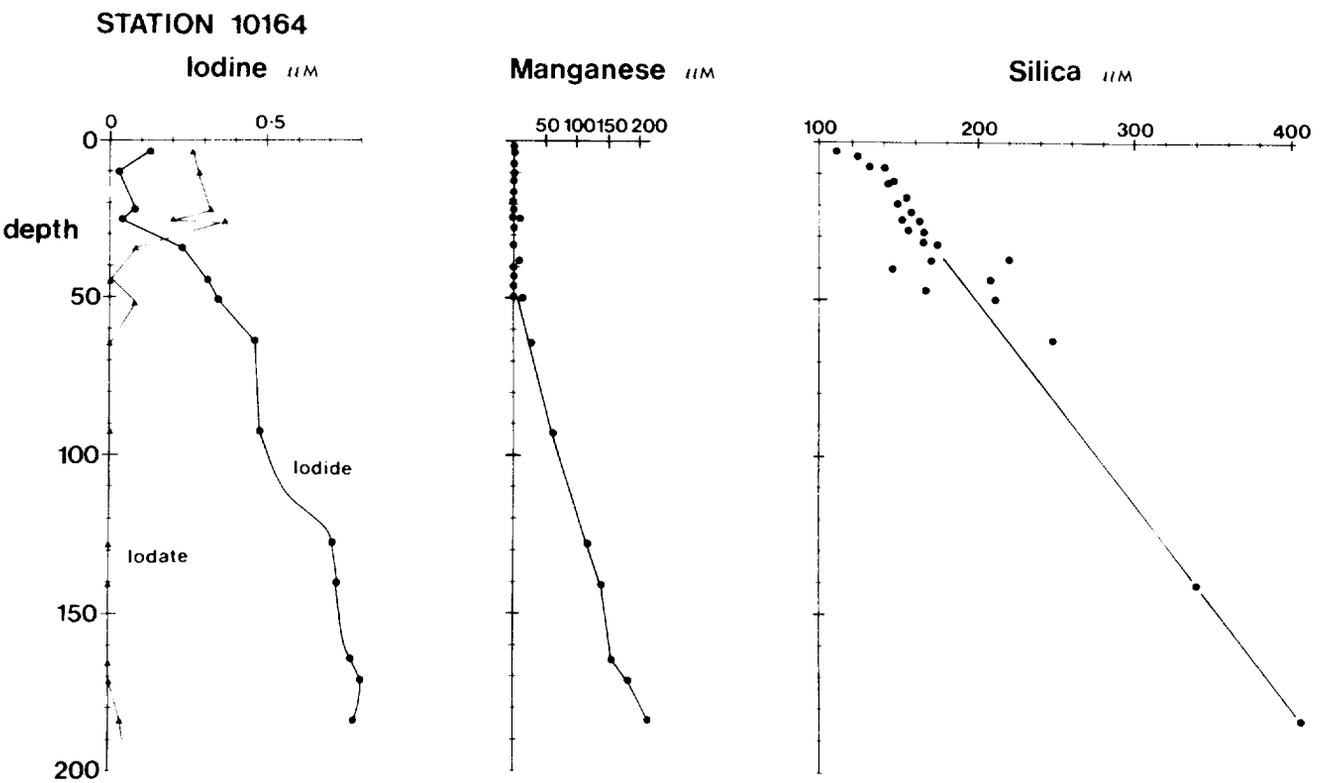
STATION 10164
Iodine µM
Manganese µM
Silica µM
0
0·5
50 100150 200
100
200
300
400
depth
0
50
100
150
200
Iodide
Iodate

Figure 3: Descriptive core logs and solid phase concentration/depth profiles for CaO, MnO, Co and Cu in cores 10163#6K and 10164#1K. The triangles indicate the values of Co and Cu typical of shale (WEDEPOHL, 1968).

DISCOVERY STATION: 10163 # 6K

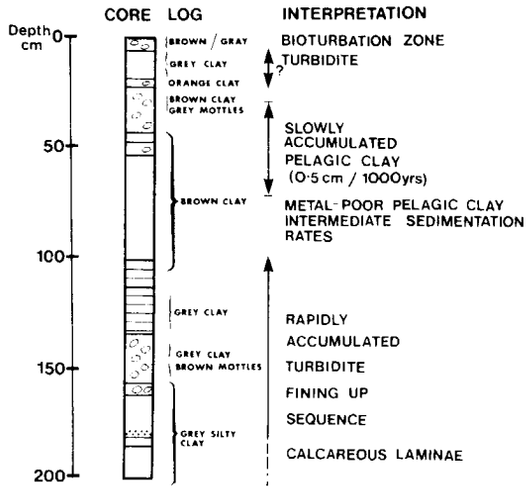

BULK SEDIMENT COMPOSITION PROFILE.

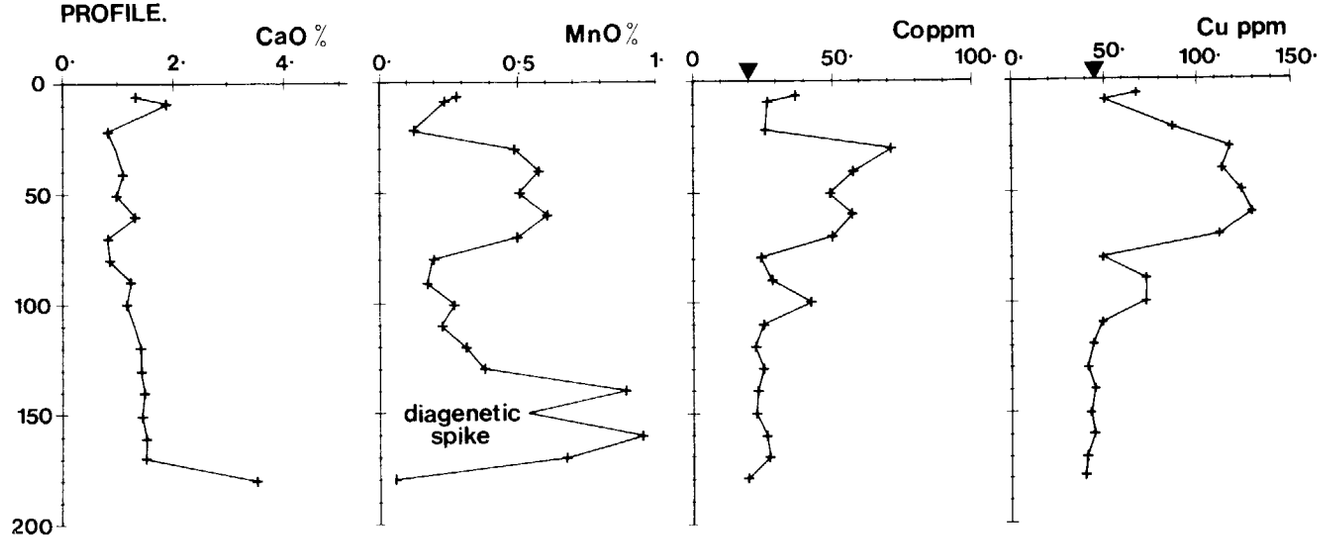

DISCOVERY STATION: 10164 # 1K

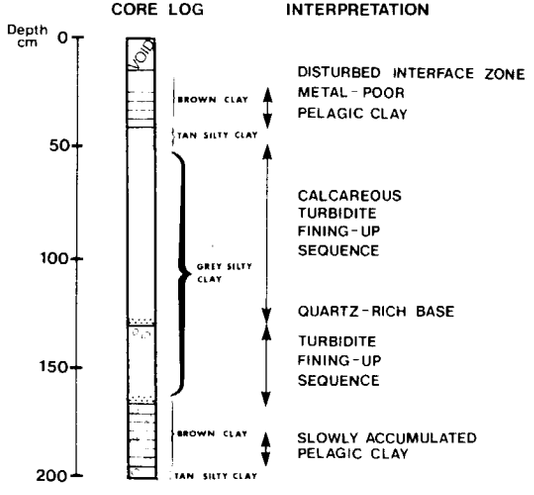

BULK SEDIMENT COMPOSITION PROFILE.

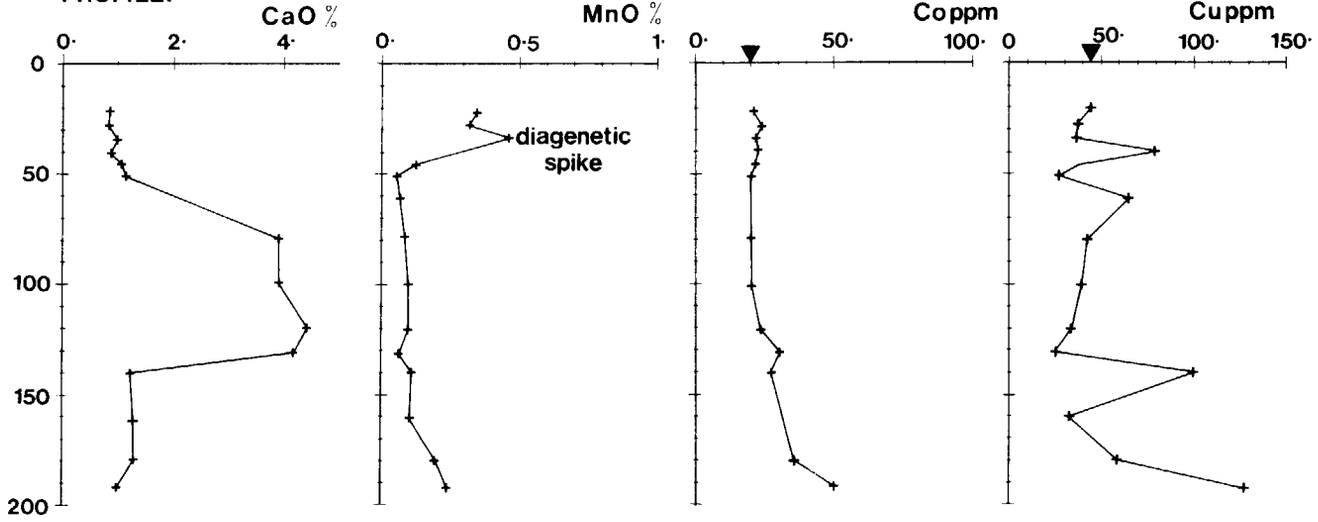

Figure 4: Core descriptions and $^{230}Th_{excess}$ data versus depth for the four box cores studied. The surface intercept (A_o) and sediment accumulation rates derived from the best-fit lines are also shown.

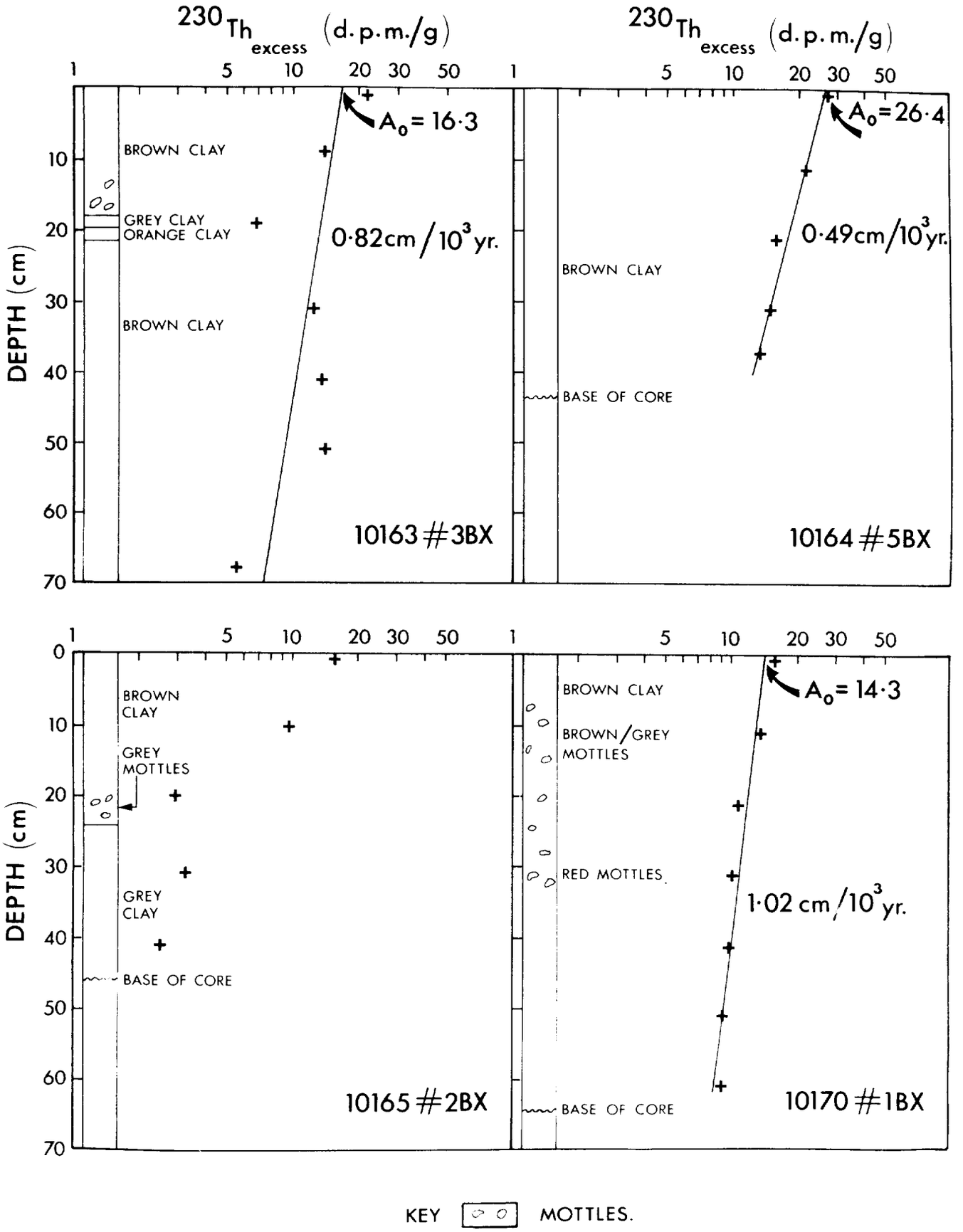
230Th excess (d.p.m./g)
1 5 10 20 30 50
DEPTH (cm)
BROWN CLAY
GREY CLAY
ORANGE CLAY
BROWN CLAY
A0 = 16·3
0·82cm / 10³yr.
10163 #3BX
230Th excess (d.p.m./g)
1 5 10 20 30 50
BROWN CLAY
BASE OF CORE
A0 = 26·4
0·49cm/10³yr.
10164 #5BX
0 10 20 30 40 50 60 70
BROWN CLAY
GREY MOTTLES
GREY CLAY
BASE OF CORE
10165 #2BX
BROWN CLAY
BROWN/GREY MOTTLES
RED MOTTLES
BASE OF CORE
A0 = 14·3
1·02 cm/10³yr.
10170 #1BX
KEY MOTTLES.

Figure 5: Core descriptions and $^{230}Th_{excess}$ data versus depth for Kasten cores 10163#6K and 10164#1K. A sediment accumulation rate can be derived only for a short portion of core 10163#6K as shown.

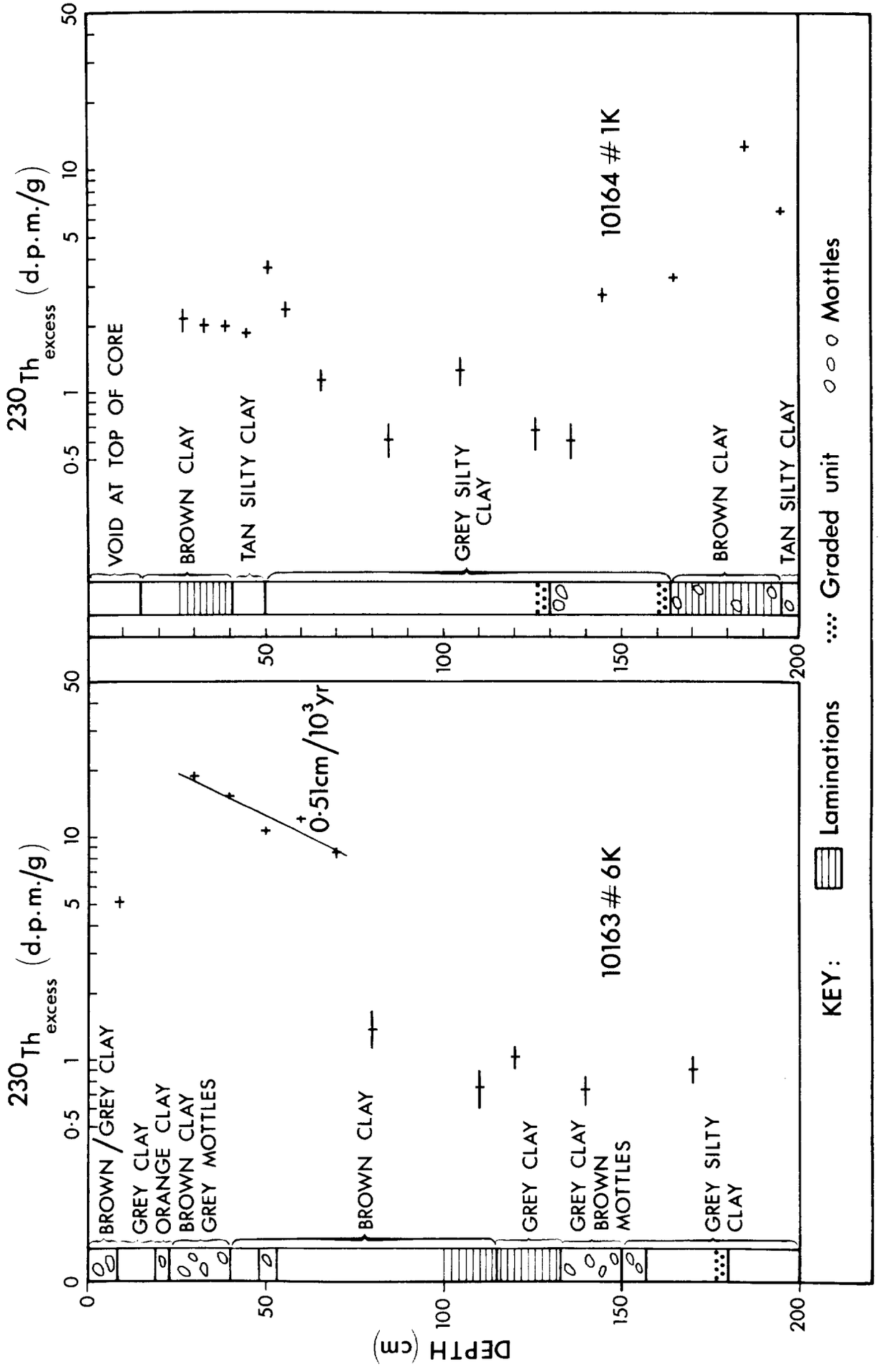
$^{230}Th_{excess}$ (d.p.m./g)
0
0·5
1
5
10
50
BROWN / GREY CLAY
GREY CLAY
ORANGE CLAY
BROWN CLAY
GREY MOTTLES
BROWN CLAY
GREY CLAY
GREY CLAY
BROWN
MOTTLES
GREY SILTY
CLAY
0·51cm/10³yr
10163 # 6K
DEPTH (cm)
50
100
150
200
VOID AT TOP OF CORE
BROWN CLAY
TAN SILTY CLAY
GREY SILTY
CLAY
BROWN CLAY
TAN SILTY CLAY
10164 # 1K
KEY:
Laminations
Graded unit
Mottles

Figure 6: Regression lines of the fluxes of the elements Mn, Fe, Co, Ni, Cu and Zn on the total mean sediment fluxes derived from the sediment accumulation rates of cores 10164#5BX, 10163#6K, 10163#3BX and 10170#1BX. The slope values, corresponding to the detrital matrix content of the element, and the intercept values, corresponding to the hydrogenous flux of the element, are also shown (see text, Section 4.4). (A similar treatment can be made for vanadium on a different scale).

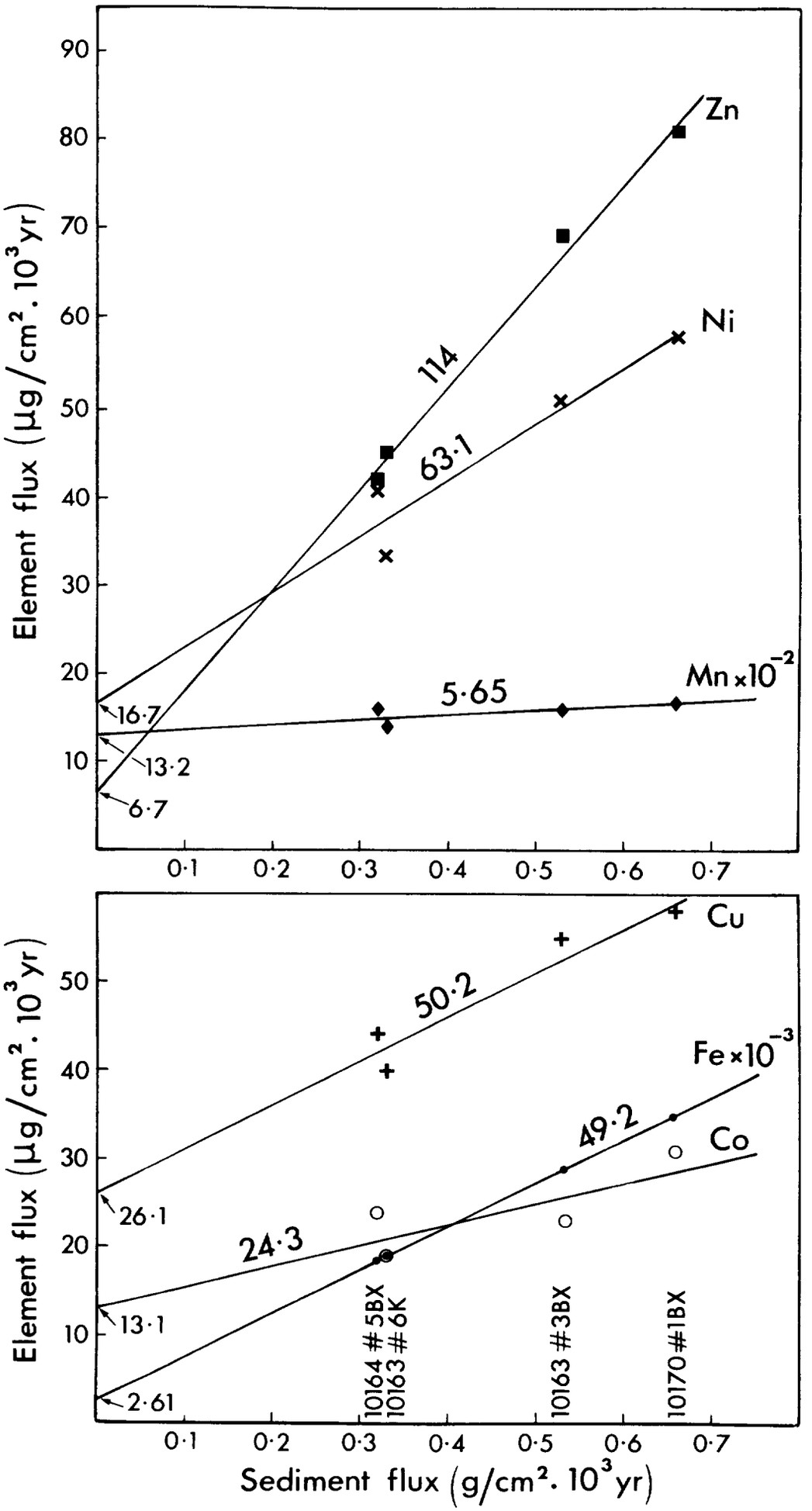
Element flux (µg/cm². 10³yr)
Zn
Ni
Mn ×10⁻²
114
63·1
5·65
16·7
13·2
6·7
Cu
Fe ×10⁻³
Co
50·2
49·2
24·3
26·1
13·1
2·61
10164 #5BX
10163 #6K
10163 #3BX
10170 #1BX
Sediment flux (g/cm². 10³yr)

Figure 7: 7a (upper): Shale normalised enrichment factors for some first row transition elements in the derived hydrogenous phase, in nodules and micronodules from the Nares Abyssal Plain area (ADDY, 1979), and in the slowly-accumulated brown clay. The Mn enrichment factor of the micronodules has been used as the fixed point for the hydrogenous phase plot.

7b (lower): The mean values of the various types of sediment identified (Table 4) and the derived detrital phase, normalised against shale and plotted for some first row transition elements. The similarity of the derived detrital phase, the grey clays and shale is apparent, as is the effect of the superimposed hydrogenous flux on the brown clay composition (see text, Section 4.3 and 4.4).

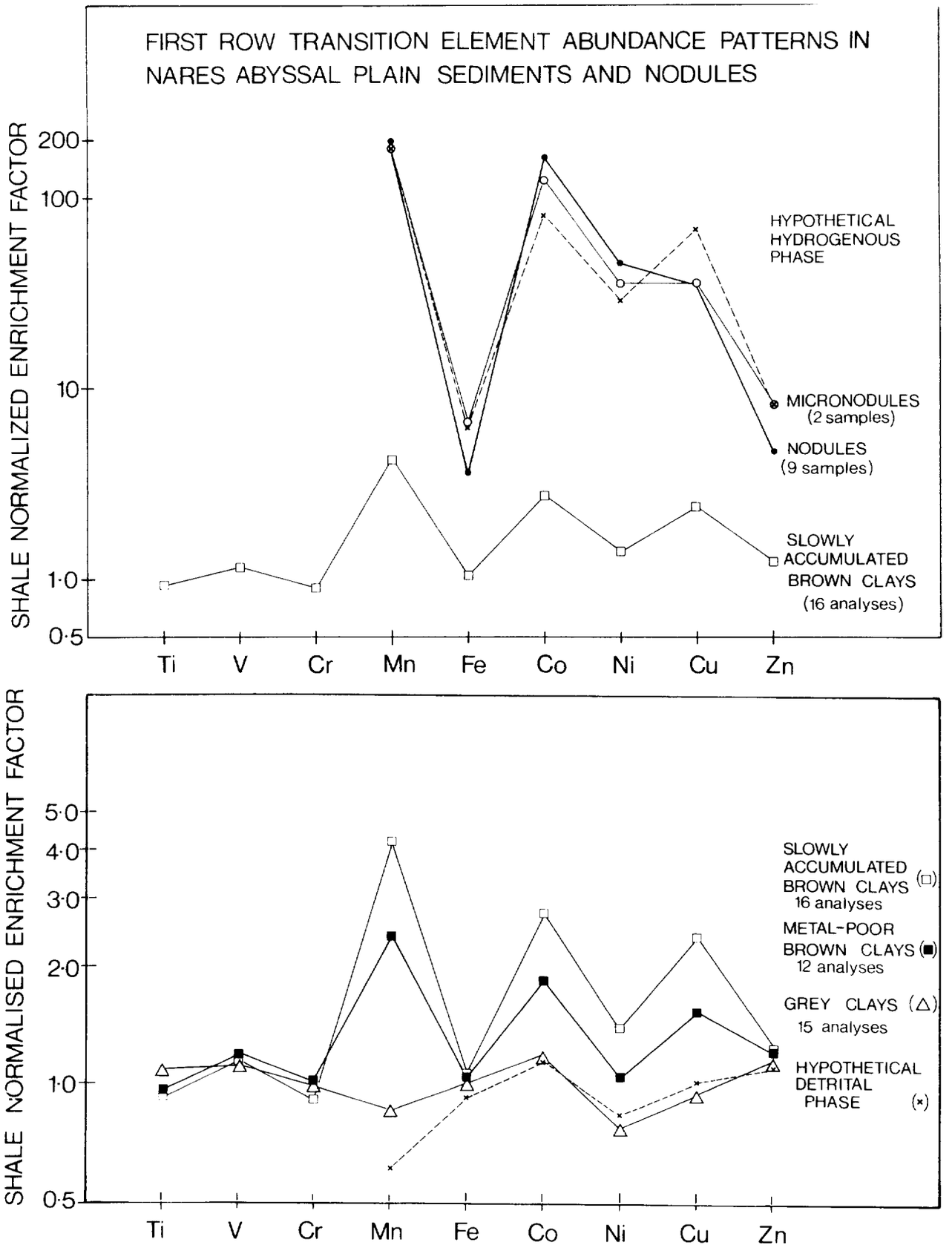
FIRST ROW TRANSITION ELEMENT ABUNDANCE PATTERNS IN NARES ABYSSAL PLAIN SEDIMENTS AND NODULES
SHALE NORMALIZED ENRICHMENT FACTOR
200
100
10
1·0
0·5
HYPOTHETICAL HYDROGENOUS PHASE
MICRONODULES (2 samples)
NODULES (9 samples)
SLOWLY ACCUMULATED BROWN CLAYS (16 analyses)
Ti V Cr Mn Fe Co Ni Cu Zn
SHALE NORMALISED ENRICHMENT FACTOR
5·0
4·0
3·0
2·0
1·0
0·5
SLOWLY ACCUMULATED BROWN CLAYS (□) 16 analyses
METAL-POOR BROWN CLAYS (■) 12 analyses
GREY CLAYS (△) 15 analyses
HYPOTHETICAL DETRITAL PHASE (×)
Ti V Cr Mn Fe Co Ni Cu Zn

APPENDIX 1

Interstitial water analysis: list of results.

10165# SG

Depth cm	Si µm	Po_4 µm	No_3 µm	ΣIodine µm	Iodide µm	Iodate µm	Manganese µm
0-2	117	4	23	0.56	0.22	0.34	-
2-4	122	8	23	0.46	0.06	0.40	0.5
4-7	138	7	26	0.61	0.12	0.49	0.6
7-9	132	4	26	0.59	0.07	0.52	0.7
9-11	-	5	22	0.68	-	-	1.4
11-13	117	5	19	0.61	0.05	0.56	0.8
13-15	113	5	22	0.76	0.15	0.61	0.8
15-17	119	2	23	0.74	0.07	0.67	1.4
17-19	121	5	22	0.74	0.04	0.70	0.9
19-21	117	5	24	0.79	0.37	0.41	0.9
21-23	123	5	22	0.84	0.15	0.70	-
25-27	123	5	24	0.96	0.14	0.82	0.4
31-33	-	4	25	0.96	0.35	0.61	0.7
35-37	130	4	24	1.02	0.21	0.82	0.5
43-45	138	5	11	0.98	0.32	0.65	1.0
47-49	160	1	-	0.56	0.50	0.06	16.6
53-55	130	5	13	0.60	0.56	0.04	-

Note. Nutrient data on this core obtained from stored samples at shore laboratory.

Depth cm	ΣIodine µm	Iodide µm	Iodate µm	Manganese µm
10163#3BX				
0-3	0.39	0.22	0.17	1.0
3-6	0.38	0.25	0.12	1.6
6-9	0.36	0.21	0.15	0.5
9-12	0.39	0.27	0.12	1.1
12-15	0.36	0.25	0.11	0.6
15-18	0.48	0.36	0.12	1.2
18-21	0.48	0.36	0.11	0.7
21-24	-	-	-	0.6
24-27	0.55	0.41	0.14	0.6
27-30	0.60	0.48	0.12	1.1
30-33	0.33	0.18	0.15	-
33-36	0.39	0.27	0.12	-
36-39	0.24	0.10	0.13	-
39-42	0.28	0.02	0.25	-
42-45	0.38	0.09	0.30	1.0
45-48	0.42	0.17	0.25	1.2
48-51	0.35	0.19	0.17	2.3
51-54	0.35	0.07	0.28	0.6
54-57	0.33	0.16	0.17	0.5
10163#3K				
11-18	0.52	-	-	-
18-25	0.49	0.44	0.05	-
46-53	-	-	-	-
53-60	-	-	-	0.3
83-90	0.52	0.33	0.20	0.8
93-100	0.60	0.53	0.09	0.8
123-130	0.52	0.26	0.25	0.7
143-150	0.66	0.51	0.15	1.2

10164#5BX				
0-3	-	-	-	0.1
3-6	0.39	0.13	0.27	0.2
6-4	-	-	0.30	0.1
9-12	0.31	0.03	0.28	0.1
12-15	-	-	0.27	0.3
15-18	-	-	-	0.3
18-21	-	-	-	-
21-24	0.40	0.08	0.32	0.3
24-27	0.24	0.04	0.20	0.1
27-30	0.24	-	-	0.1
30-33	-	-	0.18	-
33-36	0.31	0.23	0.08	0.2
36-39	-	-	-	-
39-42	0.35	-	-	0.5
42-45	0.31	0.31	0.0	0.3
45-48	0.30	-	-	0.6
48-51	-	-	-	0.4
10164#1K				
23-29	0.56	0.21	0.36	8.5
35-42	-	-	-	9.1
48-55	0.42	0.34	0.08	13.1
61-67	0.46	0.46	0.00	27.1
90-96	0.48	0.48	0.00	63.1
124-131	0.71	0.71	0.00	117.3
137-143	0.72	0.72	0.00	140.2
161-168	0.77	0.77	0.00	156.9
168-174	0.80	0.80	0.00	183.3
181-187	0.81	0.78	0.04	211.8

10165#2BX				
0-2	0.55	0.15	0.40	0.2
2-5	0.45	0.06	0.39	0.3
5-8	0.33	-	-	0.1
8-11	0.50	0.15	0.36	0.2
11-14	0.54	0.12	0.42	0.3
14-17	0.56	0.16	0.40	0.3
17-20	0.61	0.15	0.46	0.3
20-23	0.56	0.13	0.43	0.1
23-26	0.78	0.20	0.58	0.1
26-29	0.48	-	-	-
29-32	0.68	0.16	0.52	0.2
32-35	0.73	0.14	0.59	-
35-38	0.86	0.17	0.69	0.5
38-41	0.85	0.11	0.74	0.5
41-44	0.74	0.11	0.62	0.6
44-47	0.72	0.44	0.29	0.5
47-50	0.81	0.61	0.20	0.1
10170#1BX				
0-0.5	1.03	0.53	0.50	0.1
0.5-1	0.74	0.30	0.45	0.2
1-2	0.65	0.30	0.35	0.1
3-4	0.56	0.20	0.36	0.6
6-7	0.58	0.22	0.36	0.1
8-9	0.56	0.18	0.38	0.8
10-11	0.76	0.48	0.28	0.7
11-12	0.61	0.14	0.47	0.3
13-14	0.61	0.15	0.45	1.1
15-16	0.77	0.27	0.50	1.3

APPENDIX 2

Sediment analysis for major and minor elements: list of results.

(Note: Fe_2O_{3T} : all Fe expressed as Fe (111) LOI : loss on ignition at 1000°C. Org.C : organic carbon).

Sediment type	Depth Interval, cm	Major element data, % wt. dry basis														Trace element data, ppm. dry basis										
		SiO_2	Al_2O_3	Fe_2O_{3T}	MnO	MgO	CaO	K_2O	TiO_2	P_2O_5	NaCl	Na_2O	LOI	Total	CO_2	Org. C		Rb	Sr	Y	Zr	Nb	Ni	Co	V	Cr	Cu	Zn
		10163 # 3BX: water depth 5933m																								
1b	0-2	50.04	17.16	7.31	0.31	3.27	1.23	3.30	0.77	0.20	7.12	1.36	10.94	103.2	-	-		160	147	28	141	17	88	46	172	96	97	118
1b	4-6	53.33	18.11	7.78	0.31	3.17	1.29	3.58	0.81	0.21	3.20	1.70	7.78	101.28	-	-		159	138	30	146	21	88	42	174	99	87	129
1b	8-10	52.03	18.82	8.02	0.28	3.22	1.25	3.83	0.85	0.22	2.50	1.58	8.33	100.94	-	-		160	137	32	146	20	86	40	175	100	83	129
3	16-18	52.75	18.07	7.27	0.27	3.23	2.65	3.59	0.82	0.19	1.62	1.44	8.56	100.47	-	-		155	170	32	146	20	86	37	165	96	69	124
2	18-20	53.06	18.34	7.72	0.20	3.22	1.74	3.82	0.85	0.20	1.68	1.46	7.94	100.24	-	-		164	137	33	152	19	82	25	164	97	64	124
3	20-22	51.61	19.21	8.47	0.29	3.06	1.08	3.43	0.85	0.22	2.61	1.37	8.77	100.96	-	-		153	143	32	153	18	85	55	182	98	96	131
1a	30-32	51.23	19.37	8.18	0.47	3.08	0.98	3.23	0.83	0.19	2.94	1.55	8.68	100.74	-	-		148	150	29	144	17	103	51	175	96	121	135
1a	40-42	49.83	18.93	8.15	0.53	2.93	0.93	3.22	0.83	0.20	3.06	1.54	8.91	99.06	-	-		145	150	34	143	19	105	52	175	92	123	139
1a	50-52	49.87	19.12	8.10	0.56	2.94	0.91	3.23	0.83	0.20	2.91	1.64	9.88	100.20	-	-		145	148	32	144	18	119	52	175	93	127	134
1a	61-64	50.50	19.16	8.23	0.48	2.95	0.89	3.25	0.81	0.19	2.74	1.54	9.48	100.17	-	-		151	145	32	146	17	103	51	176	96	118	132
1b	66-69	50.90	19.37	8.41	0.38	3.02	0.82	3.41	0.84	0.20	2.55	1.43	9.13	100.45	-	-		157	138	30	160	21	92	42	179	99	102	130
		10164 # 5BX: water depth 5613m																								
1a	0-1	49.37	18.19	8.16	0.62	2.95	1.27	3.42	0.83	0.18	2.25	1.42	9.29	98.60	0.66	0.29		147	158	34	124	17	129	72	172	90	128	130
1a	10-12	49.43	17.93	8.15	0.64	2.88	1.90	3.33	0.80	0.17	2.45	1.50	9.13	98.53	1.68	0.08		145	185	35	123	16	127	69	168	89	130	131
1a	20-22	49.72	18.20	8.07	0.65	2.97	1.12	3.29	0.81	0.15	2.43	1.50	9.08	98.16	0.50	0.09		147	152	35	128	19	128	81	171	90	144	132
1a	30-32	49.98	18.54	8.19	0.67	2.97	0.77	3.34	0.84	0.19	2.26	1.44	8.94	98.16	0.37	0.14		142	162	33	123	17	132	71	166	88	143	132
1a	36-38	49.80	18.32	8.23	0.66	2.90	0.77	3.35	0.83	0.16	2.39	1.54	9.28	98.22	0.68	0.06		145	149	37	128	18	124	76	175	92	141	135

Sediment type	Depth Interval, cm	Major Element Data, % wt. dry basis														Trace Element Data, ppm. dry basis										
		SiO_2	Al_2O_3	Fe_2O_{3T}	MnO	MgO	CaO	K_2O	Na_2O	TiO_2	P_2O_5	NaCl	LOI	Total	CO_2	Org.C	Rb	Sr	Y	Zr	Nb	Ni	Co	V	Cr	Cu	Zn
		10164 # 1K : water depth 6221 m																								
1b	26-28	49.09	17.51	8.11	0.35	2.79	0.85	3.71	1.53	0.82	0.15	2.25	9.59	96.75	0.43	0.13	166	120	32	141	19	56	21	157	102	43	132
3	32-34	49.58	18.01	8.11	0.32	2.81	0.83	3.81	1.58	0.83	0.16	2.19	9.45	97.68	0.44	0.16	169	126	34	143	20	56	24	162	105	37	125
3	38-40	52.49	16.59	7.58	0.48	2.56	0.99	3.57	1.64	0.84	0.15	1.99	9.04	97.92	0.42	0.33	163	120	32	139	18	58	22	167	106	36	122
3	44-46	50.91	16.99	8.49	0.30	2.78	0.86	3.79	1.65	0.84	0.16	1.97	8.71	97.45	0.58	0.25	161	132	31	160	21	56	23	158	99	81	123
3	50-52	48.06	17.55	7.99	0.12	3.10	1.10	4.00	1.19	0.81	0.15	2.33	10.08	96.48	0.82	0.37	174	118	33	135	19	51	22	163	98	37	127
2	55-57	49.32	17.89	8.21	0.06	3.10	1.15	4.15	1.15	0.81	0.14	2.04	9.53	97.55	0.97	0.32	177	120	33	137	21	50	20	162	98	27	125
2	65-67	50.08	18.39	7.81	0.07	3.52	2.11	4.13	1.02	0.81	0.13	2.19	10.17	100.43	1.67	0.47	180	139	34	137	19	52	20	170	100	65	127
2	84-86	48.97	17.96	7.35	0.09	3.64	3.90	3.75	0.80	0.78	0.14	2.95	11.87	102.20	2.56	0.64	172	183	29	139	17	52	20	156	96	42	118
2	104-106	48.20	16.84	7.00	0.10	2.90	3.90	3.60	0.88	0.77	0.13	2.43	12.27	99.02	3.11	0.44	165	177	30	135	16	47	20	151	92	39	114
2	124-126	52.52	15.85	6.25	0.10	3.24	4.41	3.27	1.28	0.51	0.13	2.11	11.25	100.92	3.78	0.67	148	182	32	156	18	48	23	142	84	34	104
2	135-137	62.08	12.75	4.38	0.06	2.55	4.16	2.44	1.98	0.72	0.13	1.73	9.14	102.12	3.78	0.44	107	170	30	211	18	68	30	102	68	25	80
2	144-146	50.39	17.85	7.70	0.11	3.48	1.23	3.99	1.19	0.79	0.14	2.29	9.62	98.78	1.02	0.30	169	121	30	135	16	57	27	171	98	101	123
2	164-166	52.61	16.76	7.28	0.10	2.96	1.28	3.65	1.29	0.90	0.15	2.02	9.47	98.47	1.28	0.46	163	120	33	160	18	64	31	155	98	32	121
1a	184-186	50.00	16.89	8.09	0.20	3.16	1.28	3.67	1.37	0.78	0.15	2.64	10.36	98.59	1.30	0.33	150	132	29	135	16	67	35	149	86	58	122
1a	196-198	49.23	17.53	7.80	0.24	2.95	0.99	3.49	1.37	0.81	0.15	2.75	10.45	97.76	0.49	0.21	147	135	29	137	17	68	50	148	93	127	123

Sediment type	Depth interval, cm	Major element data, % wt. dry basis														Trace element data, ppm. dry basis									
		SiO_2	Al_2O_3	Fe_2O_{3T}	MnO	MgO	CaO	K_2O	TiO_2	P_2O_5	NaCl	Na_2O	LOI	Total	CO_2	Org. C		Rb	Sr	Y	Zr	Nb	Ni	Co	V	Cr	Cu	Zn
		10165 # 2BX: water depth 5900m																									
1b	0-1	49.13	17.82	7.80	0.27	3.80	1.19	3.46	0.78	0.13	3.41	1.20	10.20	99.19	0.74	0.46		155	131	28	132	18	73	35	165	95	75	125
3	9-11	50.28	18.04	7.80	0.26	3.60	1.23	3.74	0.82	0.17	1.79	1.44	8.76	97.93	0.92	0.26		164	134	31	138	20	68	32	167	100	66	129
3	19-21	50.94	18.32	7.45	0.32	3.59	2.50	3.87	0.83	0.16	1.87	1.45	9.21	100.51	1.44	0.29		164	153	31	137	20	59	25	156	95	56	125
2	30-32	49.53	16.83	7.54	0.15	3.48	4.60	3.47	0.75	0.14	2.10	1.15	11.56	101.30	4.83	-		156	226	29	130	20	51	20	149	95	38	117
2	40-42	48.39	17.11	7.60	0.11	3.53	5.12	3.49	0.77	0.15	1.68	1.18	10.80	99.93	2.20	-		156	217	30	133	16	51	21	149	94	31	112
		10170 # 1BX: water depth 5520m																									
3	0-1	48.36	16.71	7.49	0.27	3.24	2.36	3.23	0.79	0.19	4.21	1.40	11.47	99.72	3.00	0.05 0.12		143	166	27	127	15	73	34	162	100	84	118
3	10-12	44.19	15.28	6.75	0.27	2.83	9.10	2.47	0.68	0.18	2.30	1.00	14.37	99.42	4.27	0.96 0.94		129	360	28	122	15	70	37	146	90	78	110
3	20-22	45.78	16.36	7.12	0.28	2.86	7.38	2.82	0.71	0.17	2.10	1.04	12.72	99.34	4.67	0.53 0.48		135	303	27	128	15	77	40	155	95	81	115
3	30-32	48.46	17.20	7.74	0.34	3.07	4.05	3.30	0.76	0.16	2.01	1.22	10.15	98.46	2.32	0.34		143	216	30	136	17	88	43	170	111	87	123
3	40-42	49.48	17.20	7.86	0.45	3.28	1.97	3.55	0.79	0.17	2.36	1.36	8.83	97.30	1.12	0.19		147	161	30	134	16	104	50	169	109	98	128
1b	50-52	50.69	17.25	7.89	0.37	3.45	1.90	3.81	0.80	0.18	3.19	1.60	8.32	98.35	1.49	0.08		152	162	36	133	17	97	52	165	102	91	129
1b	60-62	51.58	17.16	7.86	0.37	3.51	1.99	3.60	0.76	0.15	2.24	1.73	8.56	99.51	1.36	0.16		153	168	32	133	16	109	73	160	99	87	128

APPENDIX 3

Radiochemical analysis: list of results

(Note: quoted uncertainties are derived from one-sigma counting statistics).

Depth cm	U ppm	Th ppm	Th/U	$\frac{^{234}U}{^{238}U}$ activity ratio	$\frac{^{230}Th}{^{232}Th}$ activity ratio	^{230}Th dpm/g	^{234}U dpm/g	$^{230}Th_{excess}$ dpm/g
10163#6K								
8-10	2.74±0.10	16.2±0.7	5.9±0.3	0.91±0.04	1.77±0.05	7.0±0.3	1.87±0.07	5.10±0.31
29-31	2.39±0.08	16.9±0.6	7.1±0.4	1.01±0.04	5.00±0.09	20.6±0.7	1.80±0.06	18.8±0.7
39-41	2.26±0.08	15.1±0.5	6.7±0.3	0.89±0.04	4.60±0.08	16.9±0.5	1.51±0.06	15.3±0.5
49-51	2.19±0.07	15.0±0.4	6.8±0.3	0.96±0.04	3.34±0.08	12.2±0.3	1.57±0.05	10.6±0.3
59-61	2.38±0.06	15.3±0.5	6.4±0.3	0.87±0.03	3.68±0.09	13.6±0.3	1.55±0.04	12.1±0.3
69-71	2.30±0.05	14.5±0.8	6.3±0.4	0.87±0.04	2.82±0.09	10.0±0.5	1.47±0.06	8.5±0.5
79-81	2.38±0.06	15.6±1.5	6.5±0.6	0.82±0.02	0.75±0.05	2.85±0.28	1.46±0.04	1.39±0.28
109-111	2.39±0.07	14.2±0.9	5.9±0.4	0.88±0.03	0.68±0.03	2.33±0.15	1.57±0.05	0.76±0.16
119-121	2.48±0.10	16.2±0.7	6.5±0.4	0.87±0.04	0.67±0.02	2.66±0.12	1.61±0.07	1.04±0.14
139-141	2.47±0.06	12.1±0.6	4.9±0.3	0.85±0.02	0.78±0.03	2.30±0.11	1.56±0.04	0.74±0.12
169-171	2.45±0.09	15.7±0.7	6.4±0.4	0.88±0.04	0.66±0.02	2.51±0.13	1.60±0.06	0.91±0.14
10163#3BX								
0-2	2.26±0.07	18.2±0.9	8.0±0.5	0.96±0.04	5.2±0.1	22.8±1.0	1.63±0.05	21.1±1.0
8-10	2.40±0.09	14.8±0.7	6.2±0.4	1.02±0.05	4.4±0.1	15.8±0.7	1.83±0.07	14.0±0.7
18-20	2.68±0.11	15.2±0.7	5.7±0.3	0.95±0.04	2.36±0.06	8.7±0.7	1.91±0.08	6.8±0.7
30-32	2.32±0.07	16.0±0.8	6.9±0.4	0.92±0.03	3.6±0.1	14.1±0.6	1.60±0.05	12.5±0.6
40-42	2.96±0.11	16.7±0.9	5.7±0.4	0.89±0.04	3.8±0.1	15.6±0.8	1.97±0.08	13.6±0.8
50-52	2.73±0.05	18.6±0.9	6.8±0.3	0.92±0.02	3.5±0.1	15.9±0.7	1.89±0.04	14.0±0.7
66-69	2.55±0.06	12.1±0.6	4.8±0.2	0.92±0.03	2.46±0.08	7.3±0.3	1.75±0.04	5.5±0.3

Depth cm	U ppm	Th ppm	$Th/_U$	$\frac{^{234}U}{^{238}U}$ activity	$\frac{^{230}Th}{^{232}Th}$ activity	^{230}Th dpm/g	^{234}U dpm/g	$^{230}Th_{excess}$ dpm/g
10164 # 1K								
26-28	2.36±0.08	13.2±0.9	5.6±0.4	0.94±0.04	1.19±0.06	3.81±0.26	1.66±0.06	2.15±0.27
32-34	2.37±0.08	15.7±0.7	6.6±0.4	0.93±0.04	0.96±0.04	3.66±0.17	1.64±0.06	2.02±0.18
38-40	2.49±0.09	14.8±0.6	5.9±0.3	0.92±0.04	1.03±0.03	3.72±0.14	1.71±0.06	2.01±0.15
44-46	2.54±0.06	12.3±0.3	4.8±0.2	0.95±0.03	1.23±0.03	3.66±0.09	1.81±0.04	1.85±0.10
50-52	2.48±0.11	14.8±0.7	6.0±0.4	0.96±0.05	1.51±0.05	5.45±0.24	1.78±0.08	3.67±0.25
55-57	2.72±0.09	15.4±0.8	5.7±0.3	0.84±0.04	1.09±0.05	4.06±0.21	1.70±0.06	2.36±0.22
65-67	3.31±0.08	13.8±0.6	4.2±0.2	0.94±0.03	1.03±0.03	3.45±0.14	2.32±0.06	1.13±0.15
84-86	4.00±0.09	14.1±0.4	3.5±0.1	0.95±0.02	1.01±0.02	3.46±0.10	2.85±0.06	0.61±0.11
104-106	2.87±0.10	13.7±0.7	4.8±0.3	0.98±0.04	1.01±0.04	3.37±0.17	2.12±0.07	1.25±0.18
124-126	3.18±0.09	11.6±0.4	3.6±0.2	0.91±0.03	1.00±0.03	2.83±0.11	2.16±0.06	0.67±0.13
135-137	2.87±0.07	9.58±0.28	3.3±0.1	1.06±0.03	1.19±0.03	2.78±0.08	2.27±0.07	0.51±0.11
144-146	2.87±0.10	14.8±0.6	5.2±0.3	0.99±0.04	1.36±0.03	4.89±0.18	2.13±0.07	2.76±0.19
164-166	2.81±0.07	13.2±0.4	4.7±0.2	0.88±0.03	1.60±0.04	5.11±0.14	1.84±0.05	3.27±0.15
184-186	2.19±0.07	14.4±0.7	6.6±0.4	0.95±0.04	4.07±0.12	14.2±0.6	1.56±0.05	12.6±0.6
196-198	2.21±0.05	10.7±0.3	4.8±0.2	0.90±0.03	3.05±0.06	7.97±0.18	1.47±0.04	6.50±0.18

Depth cm	U ppm	Th ppm	Th/U	$\frac{^{234}U}{^{238}U}$ activity ratio	$\frac{^{230}Th}{^{232}Th}$ activity ratio	^{230}Th dpm/g	^{234}U dpm/g	$^{230}Th_{excess}$ dpm/g	$^{231}Pa_{excess}$ dpm/g
10164 # 5BX									
0-1	2.59±0.09	17.6±0.6	6.8±0.3	0.90±0.04	6.66±0.13	28.4±0.8	1.73±0.06	26.7±0.8	1.07±0.11
10-12	2.54±0.07	14.6±0.8	5.7±0.4	0.97±0.03	6.61±0.21	23.5±1.1	1.84±0.05	21.7±1.1	0.76±0.08
20-22	2.37±0.07	14.8±0.8	6.2±0.4	0.93±0.03	5.05±0.16	18.2±0.9	1.65±0.05	16.6±0.9	0.44±0.06
30-32	2.60±0.06	17.1±0.4	6.6±0.2	0.88±0.03	3.95±0.07	16.4±0.4	1.71±0.04	14.7±0.4	0.36±0.08
36-38	2.57±0.07	18.4±0.6	7.2±0.3	0.91±0.03	3.42±0.06	15.3±0.5	1.76±0.05	13.5±0.5	0.14±0.05
10165 # 2BX									
0-1	2.30±0.07	16.3±0.7	7.1±0.4	1.06±0.04	4.40±0.12	17.4±0.6	1.82±0.06	15.6±0.6	
9-11	2.54±0.10	14.4±0.6	5.7±0.3	0.96±0.05	3.30±0.09	11.5±0.4	1.82±0.07	9.7±0.4	
19-21	2.64±0.07	14.5±0.6	5.5±0.3	0.91±0.03	1,34±0.05	4.73±0.20	1.80±0.05	2.93±0.21	
30-32	2.31±0.07	13.8±0.4	6.0±0.3	0.90±0.03	1.44±0.04	4.82±0.14	1.56±0.05	3.26±0.15	
40-42	2.32±0.06	13.2±0.6	5.7±0.3	0.92±0.03	1.28±0.05	4.11±0.18	1.60±0.04	2.51±0.18	
10170 # 1BX									
0-1	2.24±0.08	13.8±0.4	6.2±0.3	0.93±0.04	5.18±0.12	17.4±0.4	1.56±0.06	15.8±0.4	
10-12	2.02±0.06	12.0±0.3	5.9±0.2	0.97±0.03	5.08±0.11	14.8±0.3	1.47±0.04	13.3±0.3	
20-22	2.04±0.06	12.0±0.4	5.9±0.3	0.95±0.04	4.17±0.11	12.1±0.3	1.45±0.05	10.7±0.3	
30-32	2.32±0.06	13.2±0.4	5.7±0.2	0.97±0.03	3.62±0.08	11.6±0.3	1.69±0.05	9.9±0.3	
40-42	2.39±0.06	13.7±0.5	5.7±0.3	0.92±0.03	3.39±0.09	11.3±0.3	1.64±0.04	9.7±0.3	
50-52	2.28±0.07	12.8±0.4	5.6±0.2	0.93±0.04	3.40±0.08	10.6±0.3	1.59±0.05	9.0±0.3	
60-62	2.17±0.06	14.6±0.4	6.7±0.3	0.94±0.03	2.98±0.06	10.6±0.2	1.52±0.04	9.1±0.2	